SDAC-TR-75-15

SHORT-PERIOD P WAVE ATTENUATION ALONG VARIOUS PATHS IN NORTH AMERICA AS DETERMINED FROM P WAVE SPECTRA OF THE SALMON NUCLEAR EXPLOSION

Z. A. DER and T. W. McELFRESH

Seismic Data Analysis Center

Teledyne Geotech, 314 Montgomery Street, Alexandria, Virginia 22314

15 SEPTEMBER 1975

APPROVED FOR PUBLIC RELEASE; DISTRIBUTION UNLIMITED.

Sponsored By

the Defense Advanced Research Projects Agency

Nuclear Monitoring Research Office

1400 Wilson Boulevard, Arlington, Virginia 22209

ARPA Order No. 1620

Monitored By

VELA Seismological Center

312 Montgomery Street, Alexandria, Virginia 22314

Unclassified

SECURITY CLASSIFICATION OF THIS PAGE *(When Data Entered)*

REPORT DOCUMENTATION PAGE

READ INSTRUCTIONS BEFORE COMPLETING FORM

1. REPORT NUMBER: SDAC-TR-75-16	2. GOVT ACCESSION NO.
3. RECIPIENT'S CATALOG NUMBER	
4. TITLE (and Subtitle): SHORT-PERIOD P WAVE ATTENUATION ALONG VARIOUS PATHS IN NORTH AMERICA AS DETERMINED FROM P WAVE SPECTRA OF THE SALMON NUCLEAR EXPLOSION,	5. TYPE OF REPORT & PERIOD COVERED: Technical Rept. 1 Jul 75 – 30 Jun 76
	6. PERFORMING ORG. REPORT NUMBER
7. AUTHOR(s): Der, Zoltan A. / McElfresh, Thomas W.	8. CONTRACT OR GRANT NUMBER(s): F08606-76-C-0004; ARPA Order-1620
9. PERFORMING ORGANIZATION NAME AND ADDRESS: Teledyne Geotech, 314 Montgomery Street, Alexandria, Virginia 22314	10. PROGRAM ELEMENT, PROJECT, TASK AREA & WORK UNIT NUMBERS: VT/6709
11. CONTROLLING OFFICE NAME AND ADDRESS: Defense Advanced Research Projects Agency, Nuclear Monitoring Research Office, 1400 Wilson Blvd.-Arlington, Virginia 22209	12. REPORT DATE: 15 Sep 75
	13. NUMBER OF PAGES: 65
14. MONITORING AGENCY NAME & ADDRESS *(if different from Controlling Office)*: VELA Seismological Center, 312 Montgomery Street, Alexandria, Virginia 22314	15. SECURITY CLASS. *(of this report)*: Unclassified
	15a. DECLASSIFICATION/DOWNGRADING SCHEDULE

16. DISTRIBUTION STATEMENT *(of this Report)*

APPROVED FOR PUBLIC RELEASE; DISTRIBUTION UNLIMITED.

17. DISTRIBUTION STATEMENT *(of the abstract entered in Block 20, if different from Report)*

18. SUPPLEMENTARY NOTES

19. KEY WORDS *(Continue on reverse side if necessary and identify by block number)*

Anelastic Attenuation
P Waves
Seismic Magnitudes

20. ABSTRACT *(Continue on reverse side if necessary and identify by block number)*

Average Q values were determined for ray paths to various LRSM stations from the SALMON nuclear explosion, which was located in a salt dome in Mississippi, by taking ratios of observed P wave spectra to that of the estimated source spectrum. Most average Q values for the SALMON P wavepaths throughout the eastern North America are close to 2000 while those with the last half of their path in the western United States are typically around 400-500. These differences in Q seem to be sufficient to explain the .3-.4 — over

DD FORM 1 JAN 73 1473 EDITION OF 1 NOV 65 IS OBSOLETE

Unclassified

SECURITY CLASSIFICATION OF THIS PAGE *(When Data Entered)*

408258

(cont'd p 1473A)

magnitude differences in the teleseismic event magnitude observed in the western vs. eastern United States.

SHORT-PERIOD P WAVE ATTENUATION ALONG VARIOUS PATHS IN NORTH AMERICA AS DETERMINED FROM P WAVE SPECTRA OF THE SALMON NUCLEAR EXPLOSION

SEISMIC DATA ANALYSIS CENTER REPORT NO.: SDAC-TR-75-16
AFTAC Project Authorization No.: VELA T/6709/B/ETR

Project Title: Seismic Data Analysis Center

ARPA Order No.: 2551

ARPA Program Code No.: 6F10

Name of Contractor: TELEDYNE GEOTECH

Contract No.: F08606-76-C-0004

Date of Contract: 01 July 1975

Amount of Contract: $2,319,926

Contract Expiration Date: 30 June 1976

Project Manager: Royal A. Hartenberger
(703) 836-3882

P. O. Box 334, Alexandria, Virginia 22314

ABSTRACT

Average Q values were determined for ray paths to various LRSM stations from the SALMON nuclear explosion, which was located in a salt dome in Mississippi, by taking ratios of observed P wave spectra to that of the estimated source spectrum. Most average Q values for the SALMON P wavepaths throughout the eastern North America are close to 2000 while those with the last half of their path in the western United States are typically around 400-500. These differences in Q seem to be sufficient to explain the .3-.4 magnitude differences in the teleseismic event magnitude observed in the western vs. eastern United States.

TABLE OF CONTENTS

LIST OF FIGURES

LIST OF FIGURES (Continued)

LIST OF FIGURES (Continued)

LIST OF TABLES

INTRODUCTION

The purpose of this study is to derive rough Q values in the upper mantle for various paths in North America. Such Q values have important implications for magnitude-yield comparisons between different test sites. Such comparisons are crucial for successful monitoring of the proposed threshold test-ban treaty.

It is generally accepted now that the upper mantle in the western United States has lower Q values for both P and S waves than the mantle under the eastern part of the country (Solomon and Toksöz, 1970; Der, Massé and Gurski, 1975; Booth, Marshall and Young, 1975). In the western United States Archambeau, Flinn and Lambert (1969) derived Q and velocity structures from P waves of nuclear explosions. They have found a low Q layer coincident with the low velocity layer in the upper mantle. Magnitudes of teleseismic events measured in the western United States are in general about .3-.4 magnitude units lower than those measured in the eastern United States (Booth, Marshall, and Young, 1975; Der, Massé and Gurski, 1975). This observed difference in magnitudes is consistent with the assumption that the low Q layer is absent under the eastern United States.

The studies quoted above (with the exception of that of Archambeau et al. 1969) establish only a differential in average crust-upper mantle Q values.

Solomon, S. C. and Toksöz, M. N., 1970, Lateral variation of P and S waves beneath the United States, Bull. Seism. Soc. Am., v. 60, p. 819-838.

Der, Z. A., Massé, R. P. and Gurski, J. P., 1975, Regional attenuation of short-period P and S waves in the United States, Geophys. J. R. A. S., v. 39, p. 603-611.

Booth, D. C., Marshall, P. D., and Young, J. B., 1975, Long and short-period amplitudes from earthquakes in the range 0°-114°, Geophys. J. R. A. S., v. 39, p. 523-538.

Archambeau, C. B., Flinn, E. A., and Lambert, D. G., 1969, Fine structure of the upper mantle, J. Geophys. Res., v. 74, p. 5825-5865.

In this study we obtain absolute estimates for average Q values in the East and the West by dividing the observed spectra at stations at various distances from the event SALMON by the observed close-in spectrum. An approach used previously for explosions near the Nevada Test Site by Trembly and Berg (1968) and by Frasier and Filson (1972) was to match waveforms of the first few cycles of P waves with theoretical waveforms and to adjust Q values until sufficient agreement was achieved. Frasier and Filson also took spectral ratios using a 5 sec time window, a procedure similar to that followed in this report.

Trembly, L. D. and Berg, J. W., 1968, Seismic source characteristics from explosion-generated P waves, Bull. Seism. Soc. Am., v. 58, p. 1833-1848.

Frazier, C. W. and Filson, J., 1972, A direct measurement of Earth's short-period attenuation along a teleseismic ray path, J. Geophys. Res., v. 77, p. 3782-3787.

GENERAL CONSIDERATIONS

Amplitudes of short-period seismic body waves from a given event are influenced by both the velocity distribution in the medium and the attenuation in the medium. Waves propagating in a radially symmetrical earth can arrive at a given observation point along numerous travel paths comprising various branches of the travel time curve. At certain distances some arrivals are strongly focused or defocused depending on the velocity structure. In addition to this, local layering under the observing stations will also influence the spectrum of body wave arrivals.

Evaluation of Q would require the simultaneous adjustment of a velocity model and Q to match the amplitudes of all wave arrivals. This procedure was followed by Archambeau et al. (1969) using the ray theory approach.

Archambeau et al. used non-linear filtering to identify P arrivals, a technique which distorts the pulse shapes and amplitudes. Others have relied on identifying arrivals by making record sections of the raw or frequency filtered data and attempt to follow visually arrivals which seem to be coherent from trace to trace. This approach is highly subjective at best, and the results are far from unique. Another approach is to use generalized ray theory and try to match the observed waveforms to synthetic seismograms (Helmberger and Wiggins, 1971; Gilbert and Helmberger, 1972; Wiggins and Helmberger, 1973 and 1974; Wiggins and Madrid, 1974). There are similar wave theoretical methods which are also applicable (Fuchs and Müller, 1971).

Helmberger, D. V. and Wiggins, R. A., 1971, Upper mantle structure in mid-western United States, J. Geophys. Res., v. 76, p. 3229-3245.

Gilbert, F. and Helmberger, D. V., 1972, Generalized ray theory for a layered sphere, Geophys. J. R. A. S., v. 27, p. 57-80.

Wiggins, R. A. and Helmberger, D. V., 1973, Upper mantle structure of western United States, J. Geophys. Res., v. 78, p. 1870-1880.

Wiggins, R. A. and Helmberger, D. V., 1974, Synthetic seismogram computation by expansion in generalized rays, Geophys. J. R. A. S., v. 37, p. 73-90.

Wiggins, R. A. and Madrid, J. A., 1974, P wave train synthetic seismograms calculated by quantized ray theory, Geophys. J. R. A. S., v. 37, p. 407-422.

Fuchs, K. and Müller, G., 1971, Computation of synthetic seismograms with the reflectionty method and comparison with observation. Geophys. J. R. Astr. Soc., v. 23, p. 417-433.

Arrivals which cannot be explained by the ray approximation are considered in fitting the data to a model. The effects of Q structure have not yet been considered in the work along these lines thus far. A difficulty in using this technique is the cut and try approach used to find a suitable model to fit the data. Theoretical calculations by this method show that both sharp focusing and singularities in the amplitudes tend to be smeared out, with energy arriving continuously instead of in bursts as predicted by travel time branches derived from ray theory. This is more in agreement with actual data.

Velocity models derived by these diverse methods agree in their major features but differ considerably in detail and are not precise enough to predict amplitudes of various arrivals. Therefore, simultaneous precise adjustment of velocities and Q structure without ambiguity is not feasible. We do not wish to be involved in the various conflicting interpretations of the velocity structure; therefore, we use a simpler but cruder approach similar to that of Berzon et al. (1974) in that we ignore the exact nature of arrivals.

In order to guide our analysis of the observations, we have computed amplitude-distance relationships for a few plausible velocity and Q models using a ray-theory computer program, described in detail by Julian and Anderson (1968). This computer program derives the amplitudes of body waves taking into account the geometrical spreading and anelastic attenuation specified by Q as a function of depth for a given model. Losses at interfaces are neglected by this program, but their effect is likely to be small compared to geometrical spreading and attenuation. Besides, interface losses would constitute a common multiplicative factor, which would be irrelevant in the following discussion centered at relative differences of amplitudes due to anelastic attenuation. We realize the limitations of the ray theory approach, and some of the amplitudes computed at cusps, etc. may be grossly in error,

---

Berzon, I. S., Passechnik, I. P. and Polikarpov, A. M., 1974, The determination of P-wave attenuation values in the Earth's mantle, Geophys. J. R. A. S., v. 39, p. 603-611.

Julian, B. R. and Anderson, D. L., 1968, Travel times, apparent velocities and amplitudes of body waves, Bull. Seism. Soc. Am., v. 58, p. 339-366.

TABLE I

Parameters of the crust-upper mantle velocity and Q models used in ray calculations

TABLE I-A

Archambeaus' CIT-III

	Depth (km)	P Velocity (km/sec)	Q	
1	0.0	6.0000	2000.0	
2	14.0	6.2000	2000.0	
3	14.1	6.6000	2000.0	
4	28.0	6.700	500.0	
5	28.1	7.7200	300.0	
6	45.0	7.7100	180.0	
7	60.0	7.7100	180.0	
8	80.0	7.7100	150.0	
9	90.0	7.7100	140.0	low Q
10	120.0	7.7200	170.0	
11	130.0	7.7400	170.0	
12	140.0	7.8000	180.0	
13	146.0	7.9000	180.0	
14	148.0	8.3200	180.0	
15	170.0	8.3300	600.0	
16	180.0	8.3400	700.0	
17	200.0	8.3600	800.0	
18	250.0	8.4300	800.0	
19	300.0	8.5300	800.0	
20	350.0	8.6300	1000.0	
21	375.0	8.7300	1000.0	
22	398.0	9.1000	1600.0	
23	400.0	9.7500	1800.0	
24	450.0	9.8000	1900.0	
25	500.0	9.8500	1900.0	
26	550.0	9.9000	1900.0	
27	600.0	9.9500	1900.0	
28	630.0	10.0000	2000.0	
29	645.0	10.4300	2000.0	
30	660.0	10.9300	2000.0	
31	700.0	10.9600	2500.0	
32	760.0	11.0300	2500.0	
33	800.0	11.0850	2500.0	
34	840.0	11.1300	4500.0	
35	900.0	11.1700	4500.0	
36	980.0	11.2300	5500.0	
37	1054.0	11.2800	8000.0	
38	1100.0	11.6800	8000.0	
39	1200.0	11.8000	8000.0	
40	1300.0	11.9400	8000.0	
41	1400.0	12.0800	8000.0	
42	1500.0	12.2100	8000.0	
43	1600.0	12.3300	8000.0	
44	1800.0	12.5500	8000.0	

TABLE I-B

Canadian Shield and CIT-III Mantle

	Depth	P Velocity	Q
1	0.0	5.6400	1000.0
2	6.0	6.0000	1000.0
3	16.5	6.1500	1000.0
4	35.0	6.6000	1000.0
5	35.2	8.1000	1000.0
6	115.0	8.1200	1000.0
7	165.0	8.2500	1000.0
8	265.0	8.4000	1000.0
9	300.0	8.4500	1000.0
10	350.0	8.4900	1000.0
11	375.0	8.7300	1000.0
12	398.0	9.1000	1600.0
13	400.0	9.7500	1800.0
14	450.0	9.8000	1900.0
15	500.0	9.8500	1900.0
16	550.0	9.9000	1900.0
17	600.0	9.9500	1900.0
18	630.0	10.0000	2000.0
19	645.0	10.4300	2000.0
20	660.0	10.9300	2000.0
21	700.0	10.9600	2500.0
22	760.0	11.0300	2500.0
23	800.0	11.0850	2500.0
24	840.0	11.1300	4500.0
25	900.0	11.1700	4500.0
26	980.0	11.2300	5500.0
27	1054.0	11.2800	8000.0
28	1100.0	11.6800	8000.0
29	1200.0	11.8000	8000.0
30	1300.0	11.9400	8000.0
31	1400.0	12.0800	8000.0
32	1500.0	12.2100	8000.0
33	1600.0	12.3300	8000.0
34	1800.0	12.5500	8000.0

TABLE I-C

Massé's Basin and Range Model

	Depth	P Velocity	Q	
1	0.0	6.0000	2000.0	
2	1.5	6.0100	2000.0	
3	20.0	6.0100	1000.0	
4	20.0	6.9100	1000.0	
5	31.4	6.9100	500.0	
6	31.4	7.4900	500.0	
7	37.0	7.4900	500.0	
8	37.1	7.8000	500.0	
9	48.8	7.8000	350.0	
10	48.9	7.7000	350.0	
11	55.0	7.7000	200.0	
12	79.0	7.7000	160.0	
13	84.0	7.7000	140.0	low Q
14	105.0	7.7000	150.0	
15	120.0	7.7000	165.0	
16	140.0	7.8400	180.0	
17	151.0	8.0750	200.0	
18	153.0	8.3450	200.0	
19	170.0	8.3500	550.0	
20	290.0	8.3800	800.0	
21	307.0	8.4500	800.0	
22	314.0	8.6000	800.0	
23	314.8	8.7500	800.0	
24	320.0	8.8000	800.0	
25	330.0	8.8050	800.0	
26	400.0	8.8400	1800.0	
27	410.0	8.8450	1850.0	
28	415.0	8.8450	1850.0	
29	420.0	8.9500	1900.0	
30	422.0	9.6250	1900.0	
31	430.0	9.6400	1900.0	
32	470.0	9.6500	1900.0	
33	500.0	9.8500	1900.0	
34	550.0	9.9000	1900.0	
35	600.0	9.9500	1900.0	
36	630.0	10.0000	2000.0	
37	645.0	10.4300	2000.0	
38	660.0	10.9300	2000.0	
39	700.0	10.9600	2500.0	
40	760.0	11.0300	2500.0	
41	800.0	11.0850	2500.0	
42	840.0	11.1300	4500.0	
43	900.0	11.1700	4500.0	
44	980.0	11.2300	5500.0	
45	1054.0	11.2800	8000.0	
46	1100.0	11.6800	8000.0	
47	1200.0	11.8000	8000.0	
48	1300.0	11.9400	8000.0	
49	1400.0	12.0800	8000.0	
50	1500.0	12.2100	8000.0	
51	1600.0	12.3300	8000.0	
52	1800.0	12.5500	8000.0	

TABLE I-D

Massé's EUS Model and CANSD Q Model

	Depth (km)	P Velocity (km/sec)	Q
1	0.0	5.1700	1000.0
2	4.7	5.1700	1000.0
3	4.7	6.2200	1000.0
4	21.8	6.2200	1000.0
5	21.8	7.1400	1000.0
6	42.2	7.1400	1000.0
7	42.2	8.0600	1000.0
8	72.6	8.0600	1000.0
9	72.7	8.1000	1000.0
10	73.5	8.2000	1000.0
11	77.5	8.3700	1000.0
12	93.5	8.3700	1000.0
13	94.0	8.0500	1000.0
14	107.0	7.9800	1000.0
15	107.0	8.4300	1000.0
16	325.0	8.4350	1000.0
17	328.0	8.4500	1000.0
18	328.5	8.5500	1000.0
19	328.6	8.7700	1000.0
20	332.5	8.7800	1000.0
21	410.0	8.7830	1800.0
22	420.0	8.8100	1800.0
23	425.0	8.8470	1800.0
24	430.0	8.9500	1850.0
25	432.0	9.6250	1850.0
26	440.0	9.6400	1900.0
27	590.0	9.6470	1900.0
28	610.0	9.7200	1900.0
29	670.0	10.2000	2100.0
30	695.0	10.5200	2400.0
31	707.0	10.8000	2500.0
32	710.0	11.2400	2500.0
33	800.0	11.2600	2500.0
34	840.0	11.1300	4500.0
35	900.0	11.1700	4500.0
36	980.0	11.2300	5500.0
37	1054.0	11.2800	8000.0
38	1100.0	11.6800	8000.0
39	1200.0	11.8000	8000.0
40	1300.0	11.9400	8000.0
41	1400.0	12.0800	8000.0
42	1500.0	12.2100	8000.0
43	1600.0	12.3300	8000.0
44	1800.0	12.5500	8000.0

but we are interested only in the general behavior of amplitude distance relationships as functions of Q structure. The accuracy of the ray theory approach is sufficient to simulate the general behavior of such relationships. We have computed travel times and penetration depths of rays with various takeoff angles in four crust-upper mantle models. The P velocity and Q values for these models are given in Table I. We included a low Q layer in all models associated with the western United States and kept the Q high in models characteristic of the EUS or shield type structures. Amplitudes for the various travel time branches for these models were computed at three frequencies: 0.5, 1 and 2 cps; in addition, amplitudes were computed without attenuation. The results of these calculations are shown in Figures 1 to 4, indicating the nature of the signal amplitude variations to be expected for a set of plausible models. The several branches in the attenuation plots denoted by different symbols correspond to branches in the travel time curve for each model. The computer program which made the plot defines a new branch whenever the sign of the distance increment changes when the takeoff angles are incremented. These small "branches" are artifacts of the analytical approximations in the velocity-depth function used by this program. The reader should therefore ignore the symbols and consider only the general nature of the amplitude-distance behavior.

The first in each set of amplitude plots for each model is computed without attenuation taking into account the geometrical spreading only. The second amplitude plot is for the wave period T=.5 second taking Q into account. Comparison of the two plots shows that beyond a certain distance (400-1400 km) depending on the particular velocity model the amplitudes decrease drastically due to the penetration of the rays into the low velocity - (low Q) layer in the models where such a layer is specified. In models appropriate to the Eastern United States (EUS) such decrease is less drastic due to the absence of low velocity (low Q) layer. The last two amplitude plots for each model is for the wave period of 1 and 2 seconds for which the attenuation effect is less pronounced.

The above results suggest that a low Q layer will be indicated by a sharp falloff of the general amplitude level of arrivals at a distance where the waves penetrate the layer. If no low Q layer is present, the amplitude

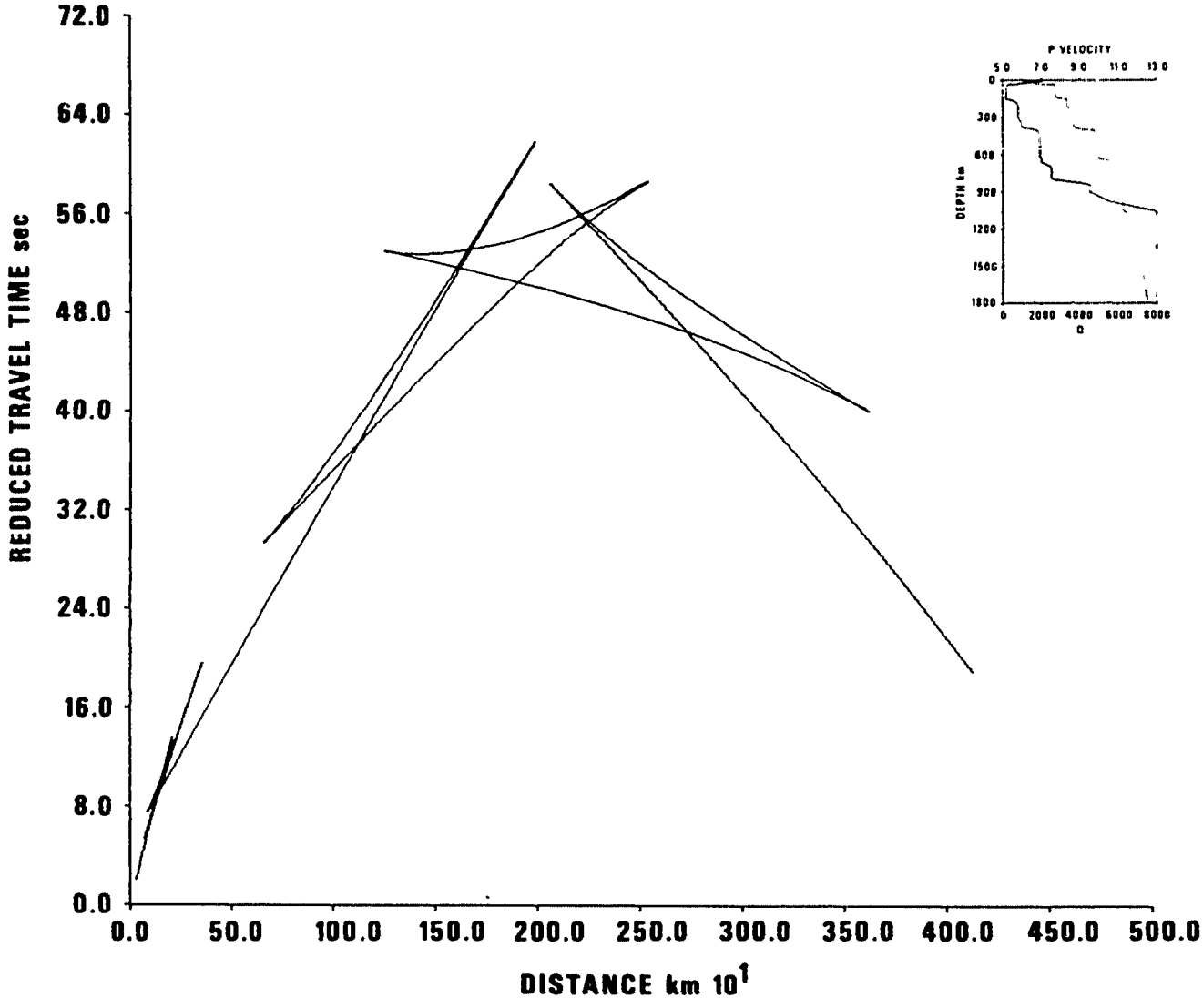

Figure 1a. Travel times for Archambeau's CIT III velocity and Q models for the Western United States.

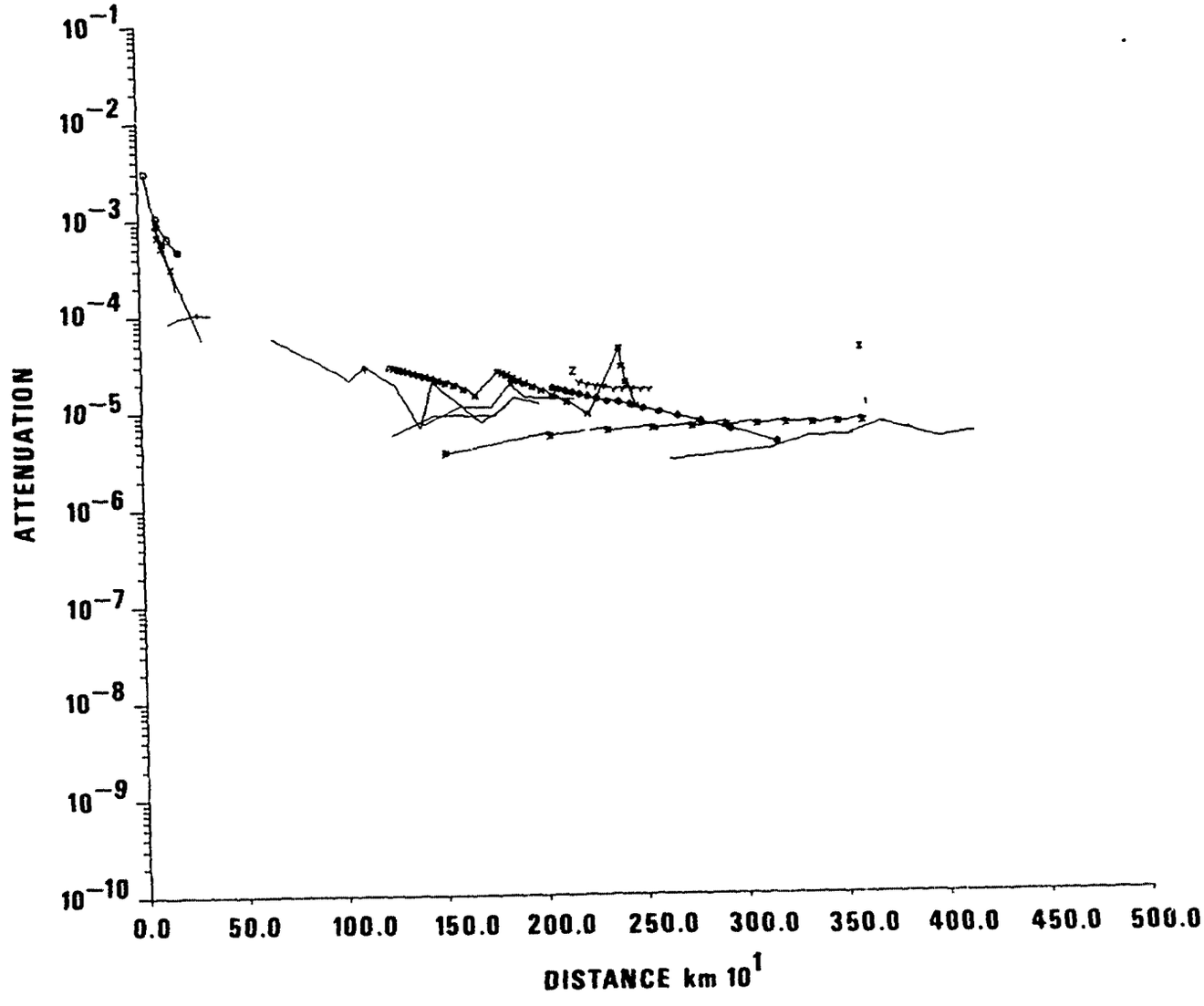

Figure 1b. Amplitudes for Archambeau's CIT III velocity and Q models for the western United States. Without attenuation.

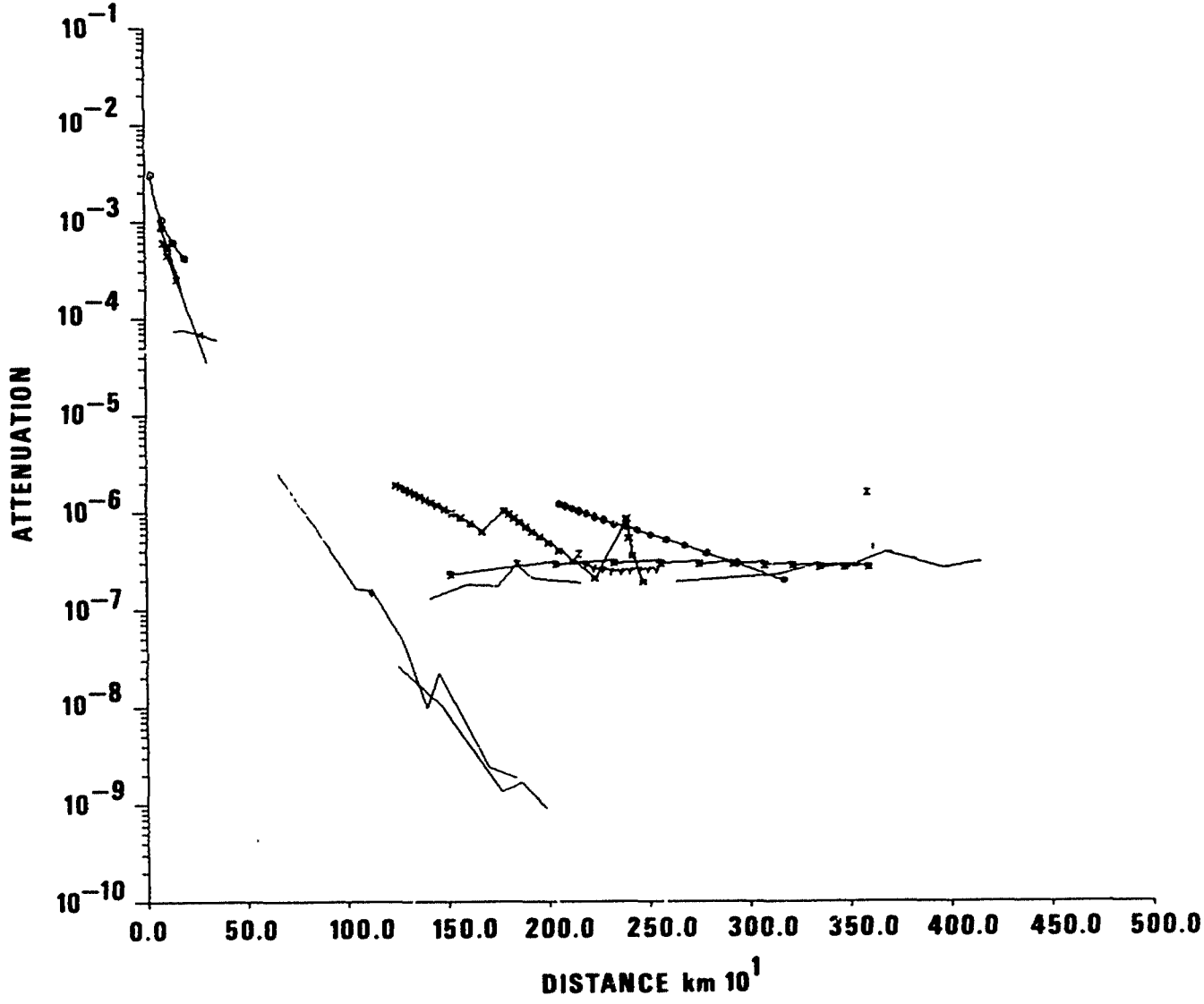

Figure 1c. Amplitudes for Archambeau's CIT III velocity and Q models for the western United States. With attenuation at the period of T = .5 sec.

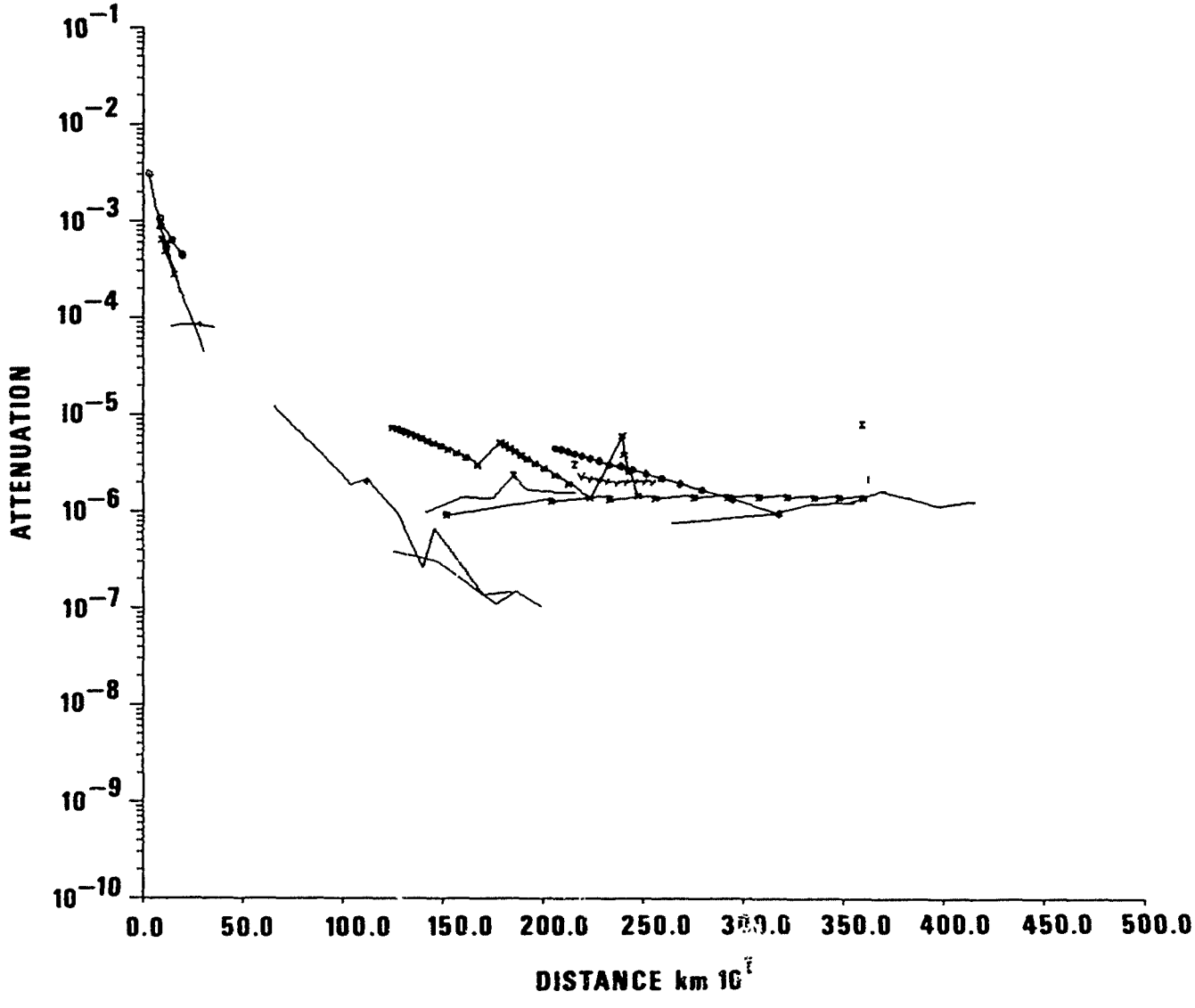

Figure 1d. Amplitudes for Archambeau's CIT III velocity and Q models for the western United States. With attenuation at the period of T = 1 sec.

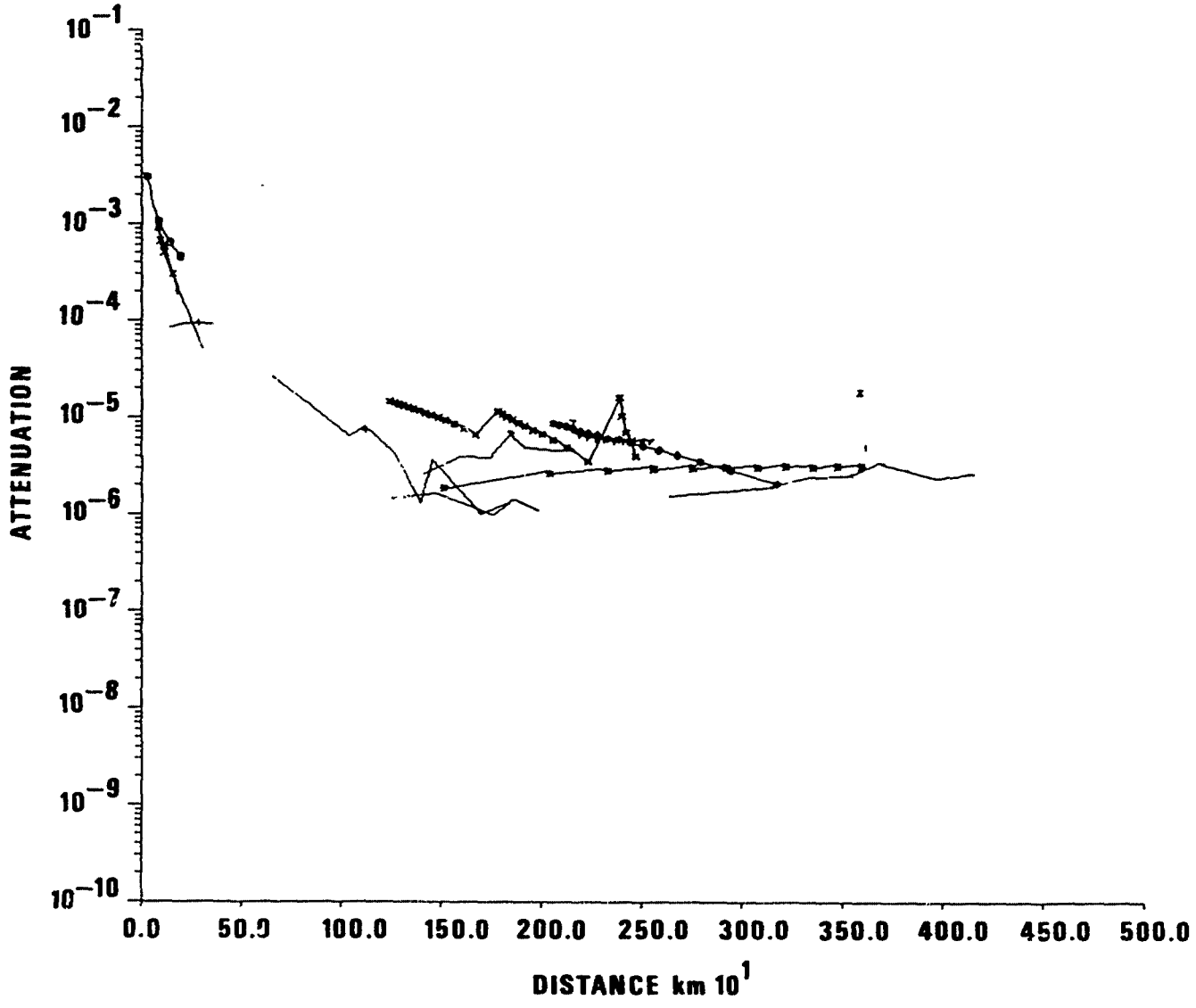

Figure 1e. Amplitudes for Archambeau's CIT III velocity and Q models for the western United States. With attenuation at the period of T = 2 sec.

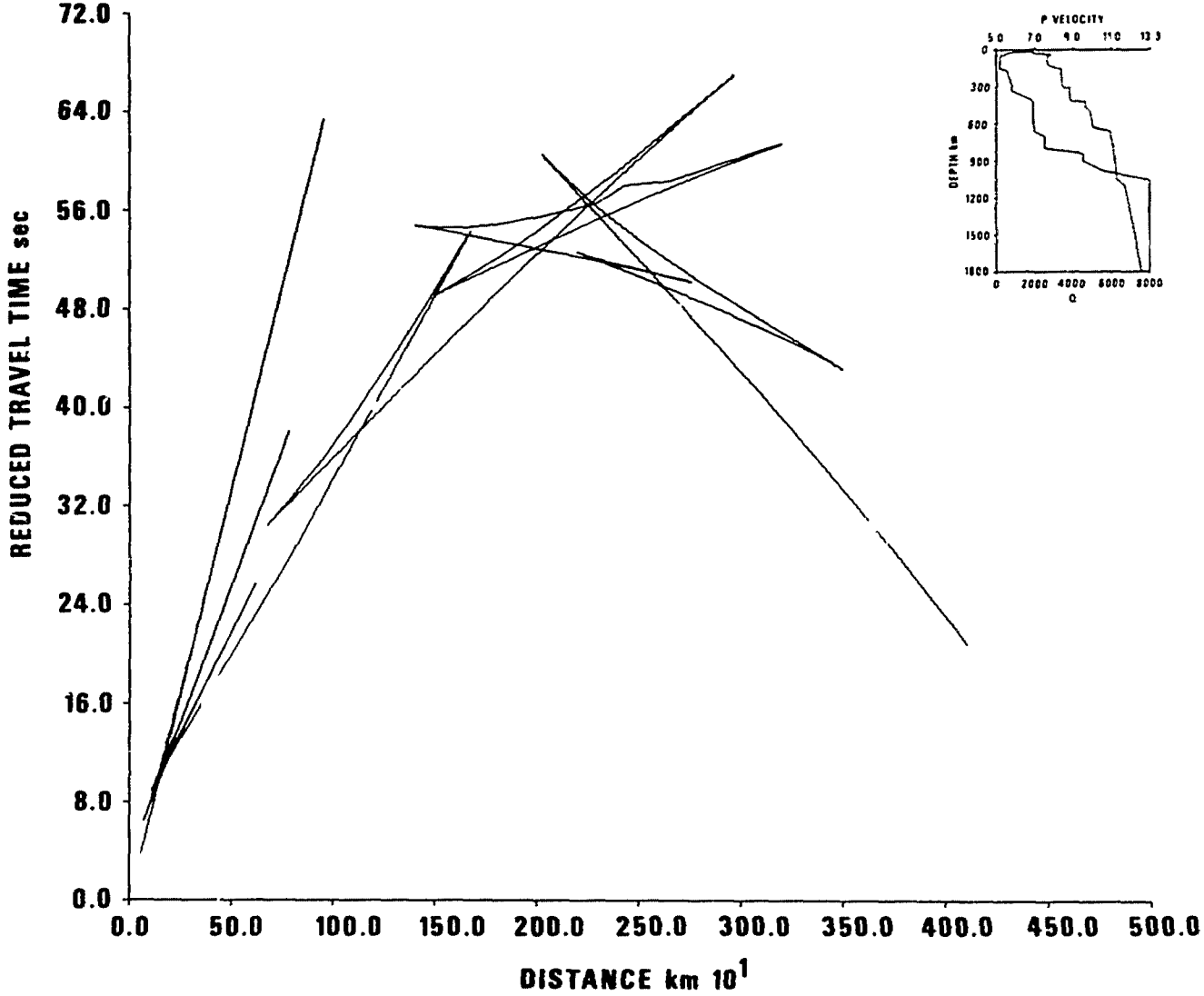

Figure 2a. Travel times for Massé's Basin and Range model with Archambeau's Q model.

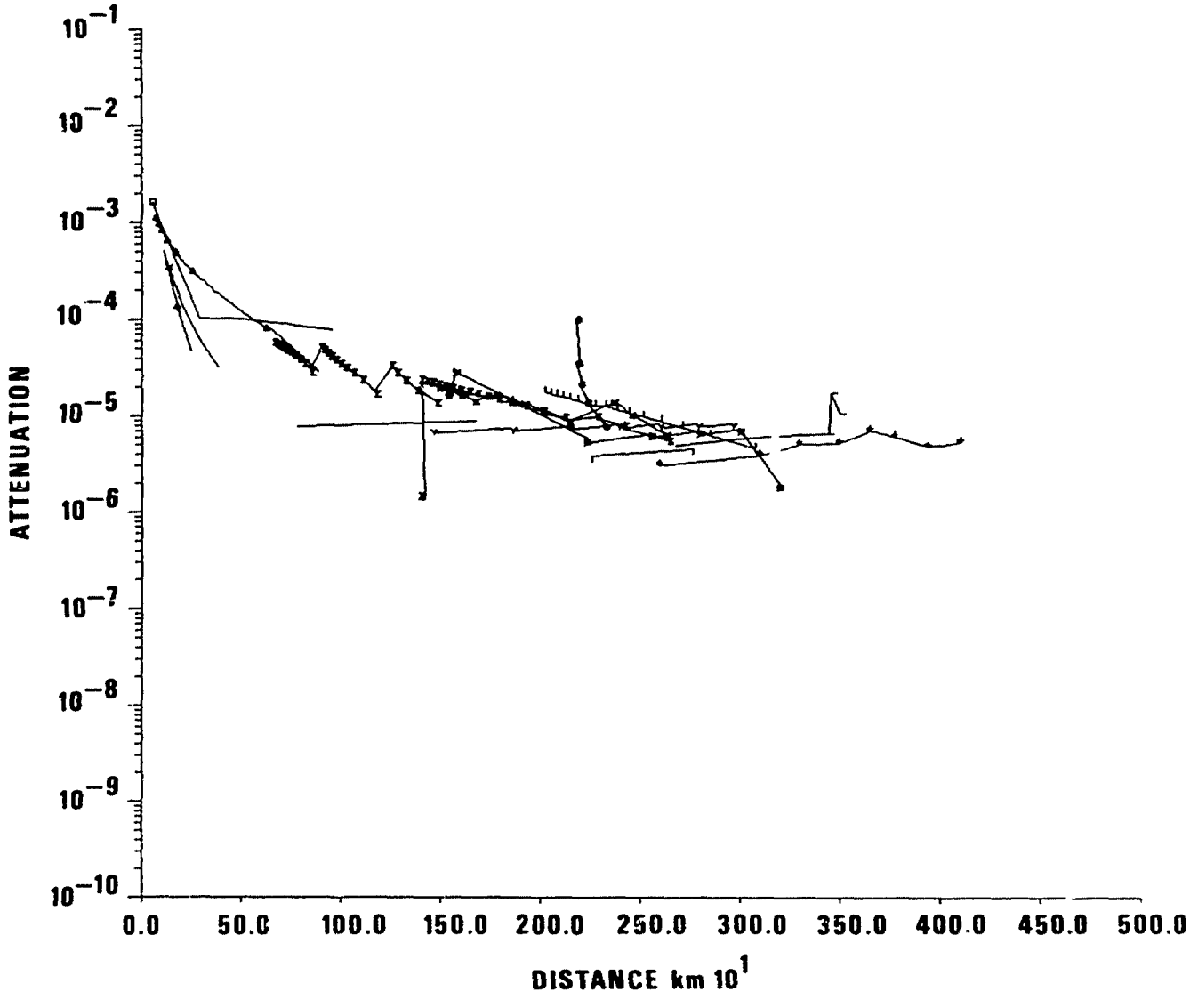

Figure 2b. Amplitudes for Massé's Basin and Range model with Archambeau's Q model. Without attenuation.

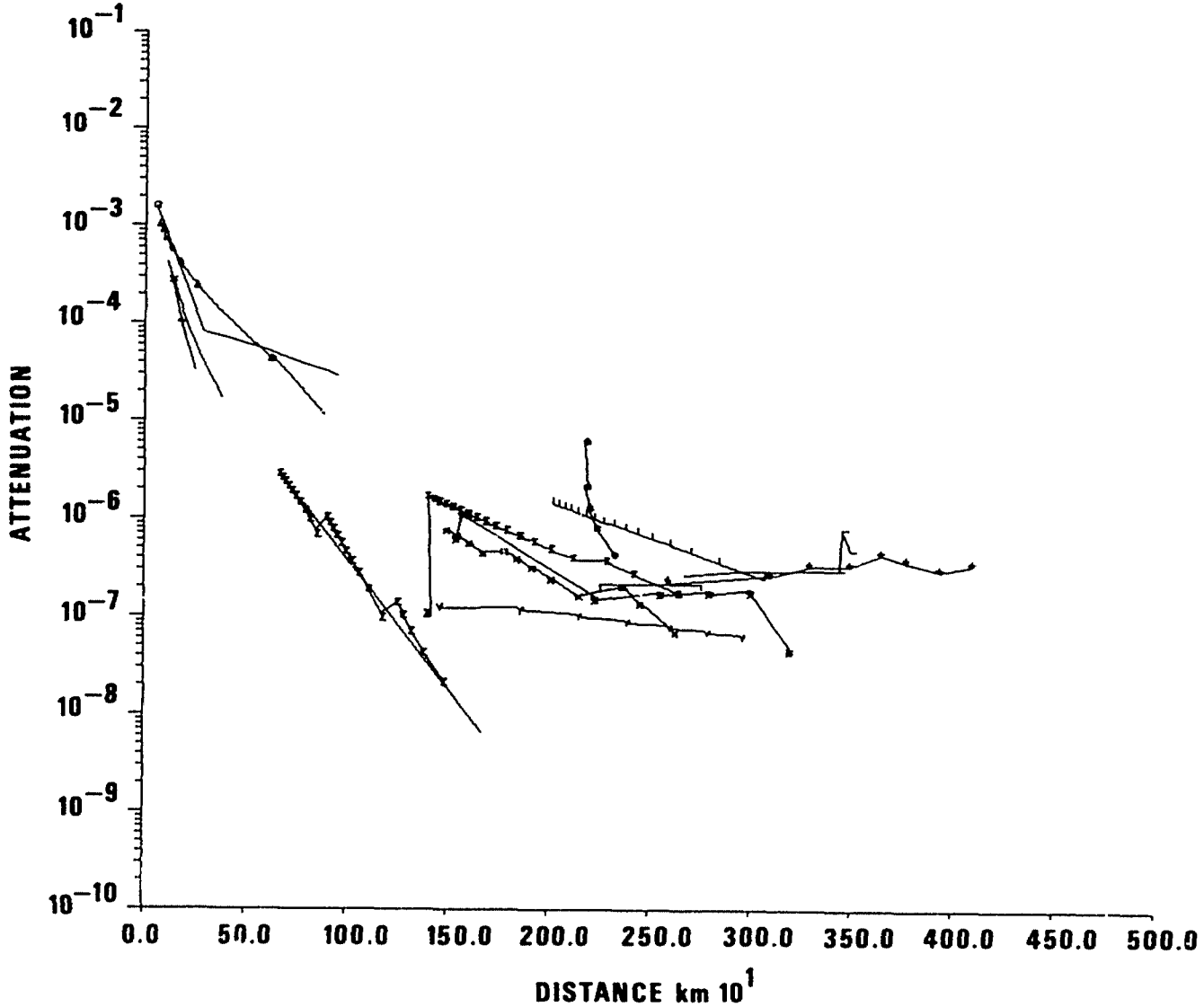

Figure 2c. Amplitudes for Massé's Basin and Range model with Archambeau's Q model. With attenuation at the period of T = .5 sec.

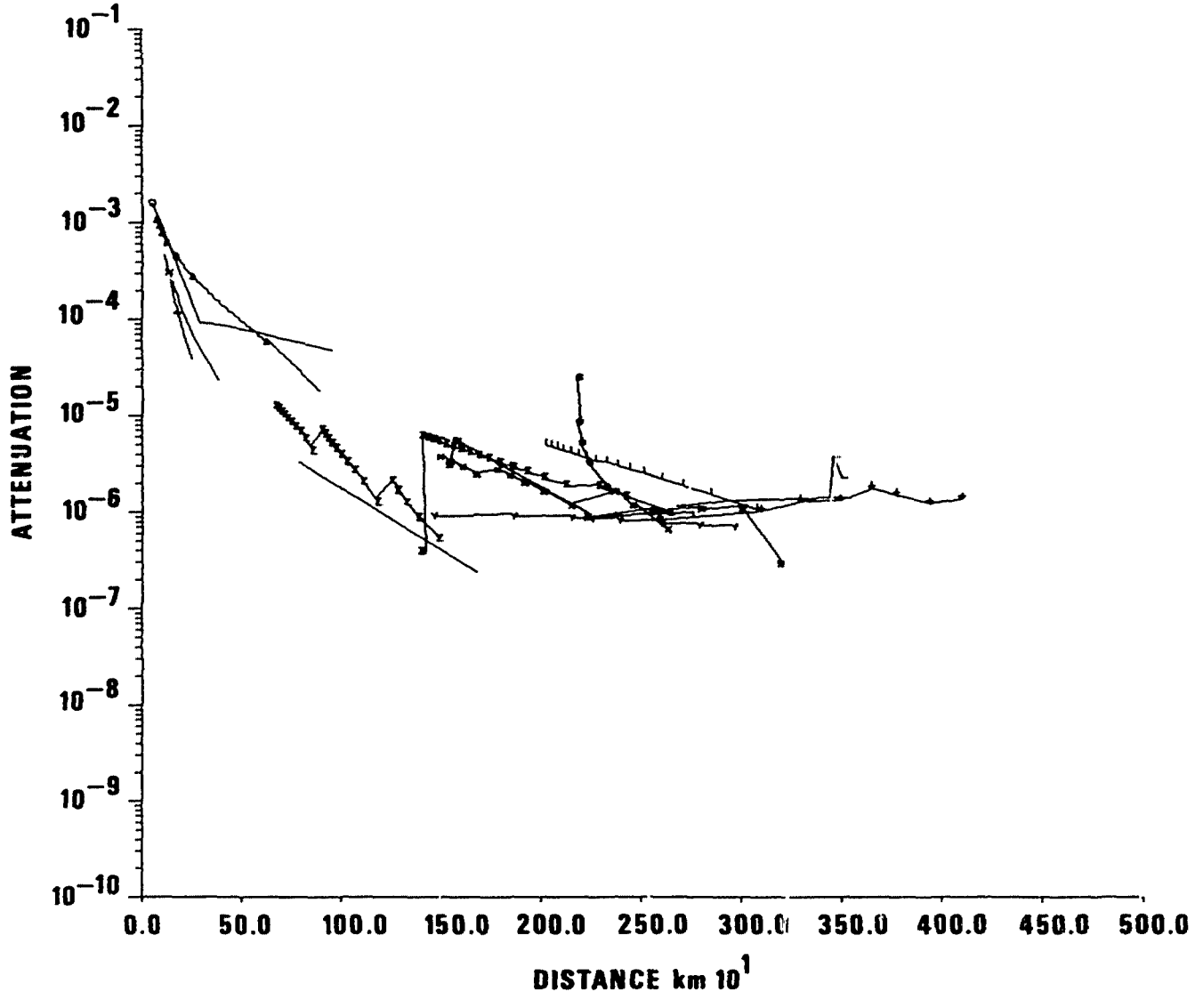

Figure 2d. Amplitudes for Massé's Basin and Range model with Archambeau's Q model. With attenuation at the period of T = 1 sec.

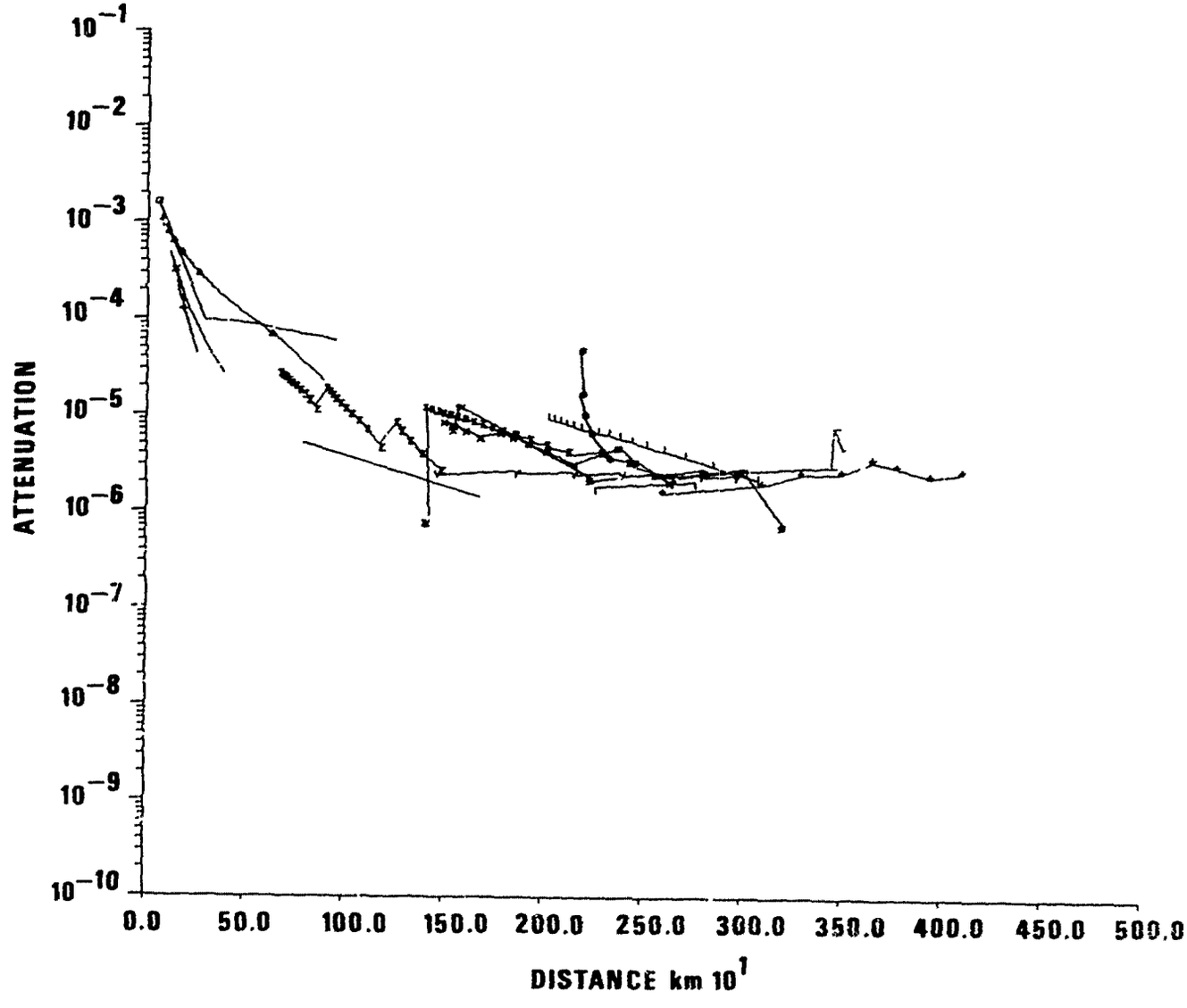

Figure 2e. Amplitudes for Massé's Basin and Range model with Archambeau's Q model. With attenuation at the period of T = 2 sec.

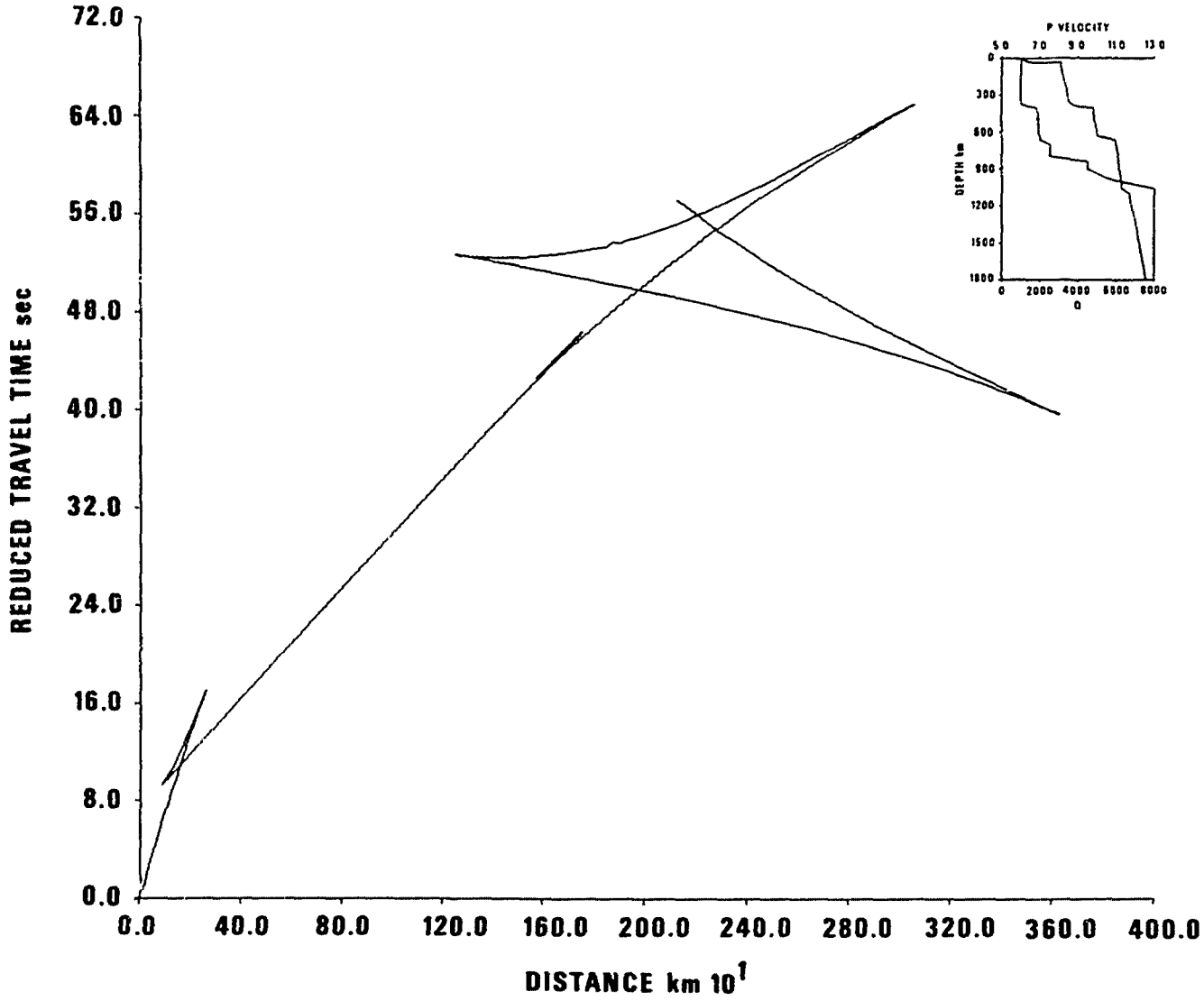

Figure 3a. Travel times for Brune and Dorman's Canadian shield model merged with CIT III at greater depth. High Q in the upper mantle.

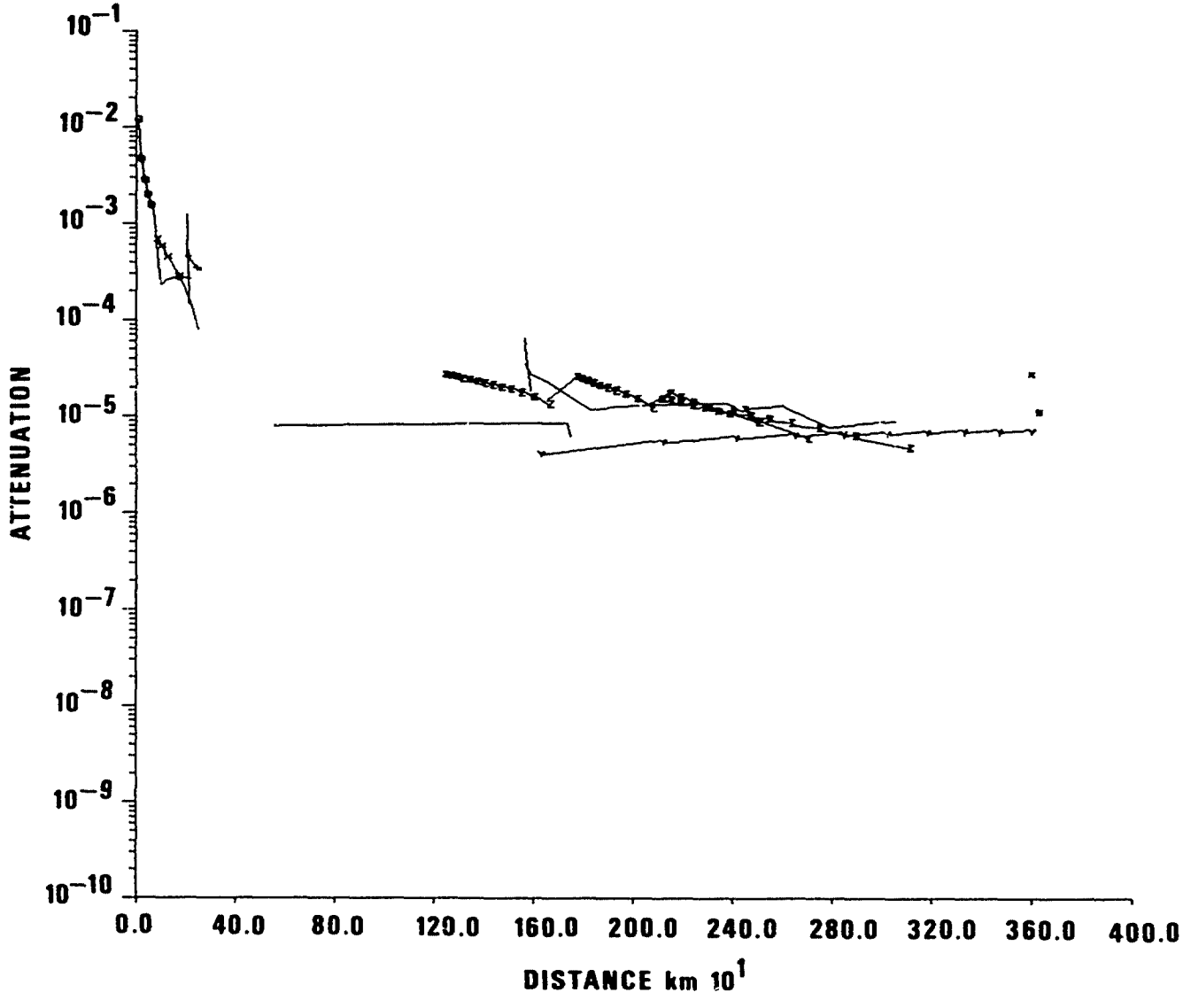

Figure 3b. Amplitudes for Brune and Dorman's Canadian shield model merged with CIT III at greater depth. High Q in the upper mantle. Without attenuation.

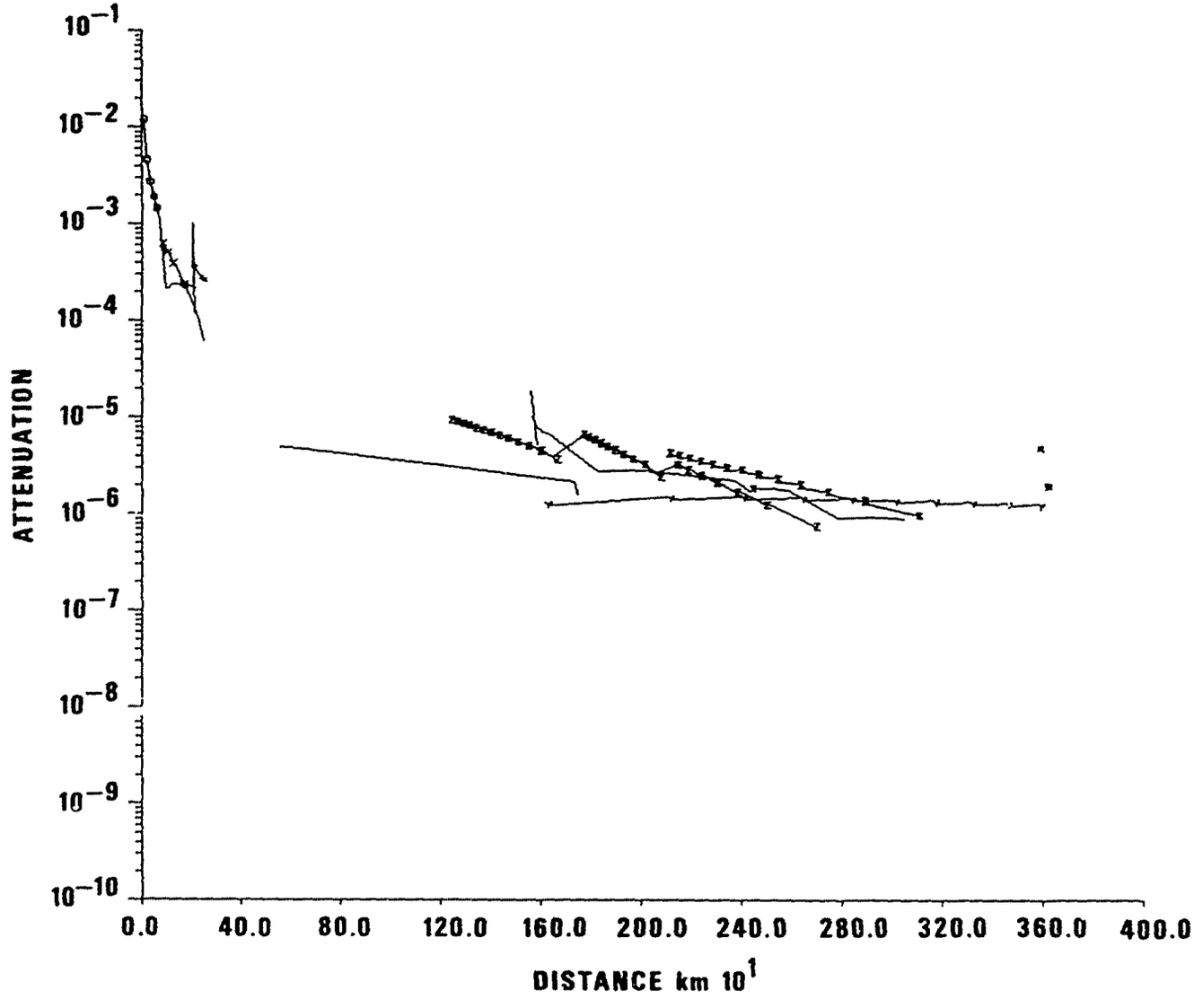

Figure 3c. Amplitudes for Brune and Dorman's Canadian shield model merged with CIT III at greater depth. High Q in the upper mantle. With attenuation at the period of T = .5 sec.

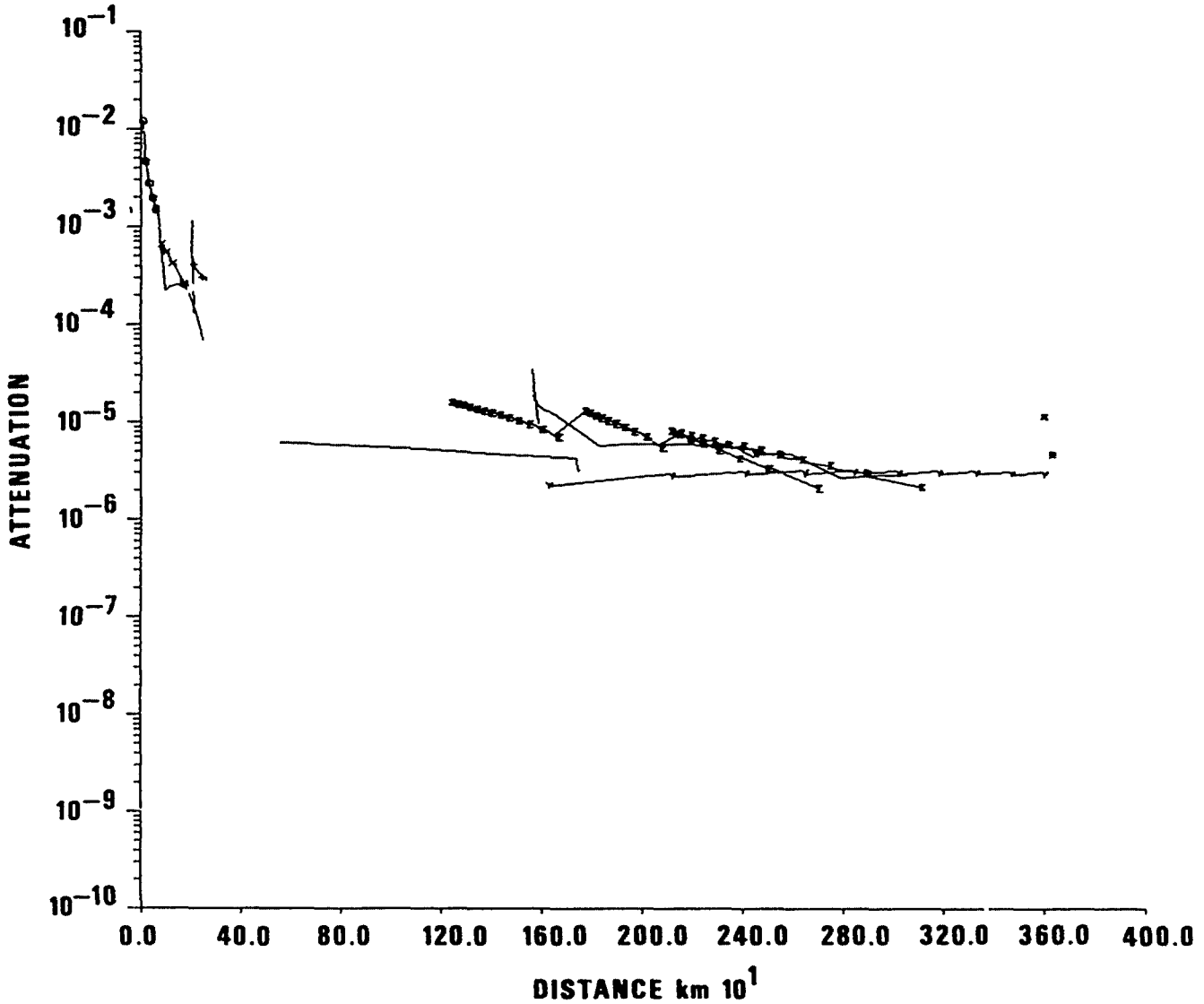

Figure 3d. Amplitudes for Brune and Dorman's Canadian shield model merged with CIT III at greater depth. High Q in the upper mantle. With attenuation at the period of T = 1 sec.

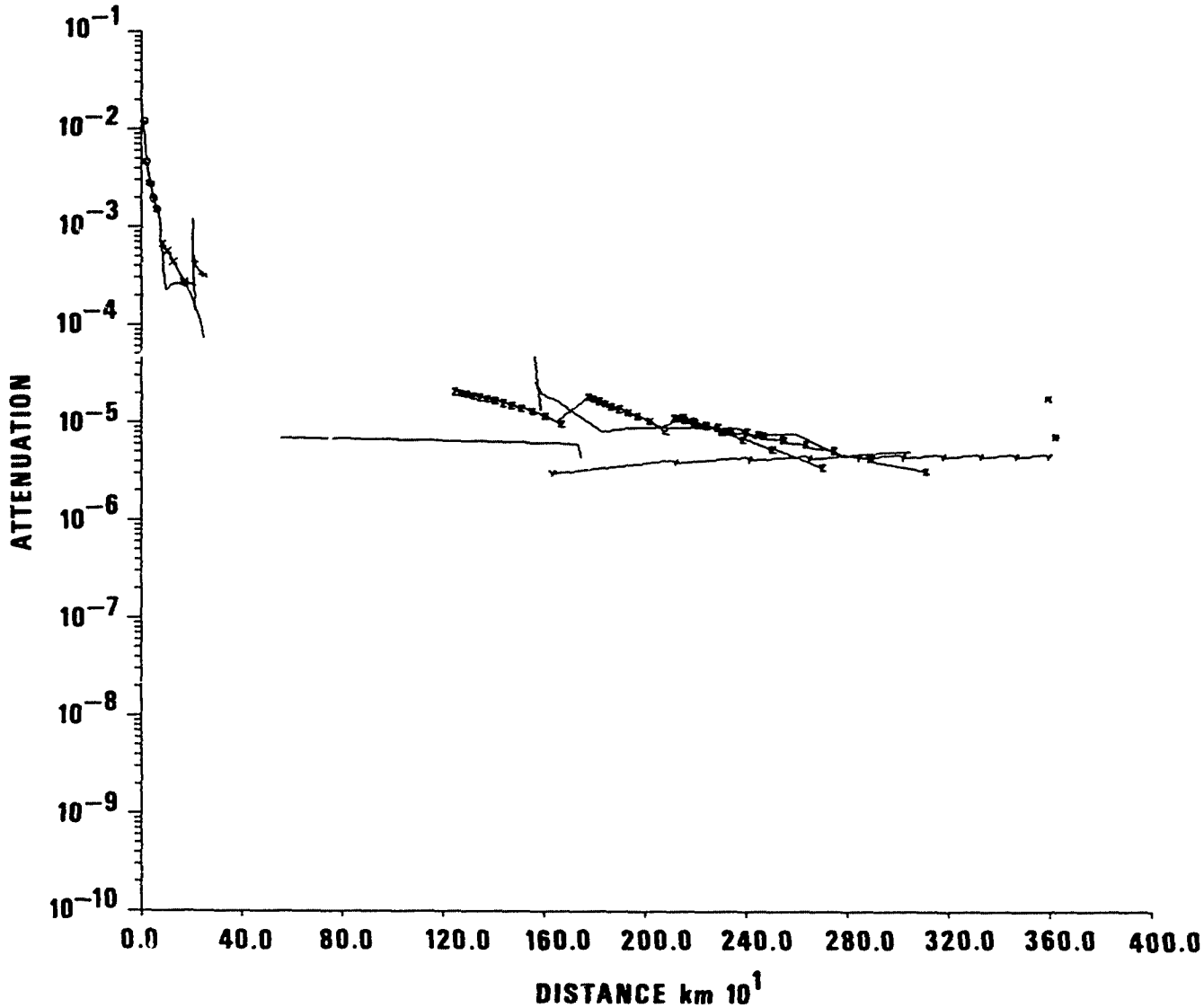

Figure 3e. Amplitudes for Brune and Dorman's Canadian shield model merged with CIT III at greater depth. High Q in the upper mantle. With attenuation at the period of T = 2 sec.

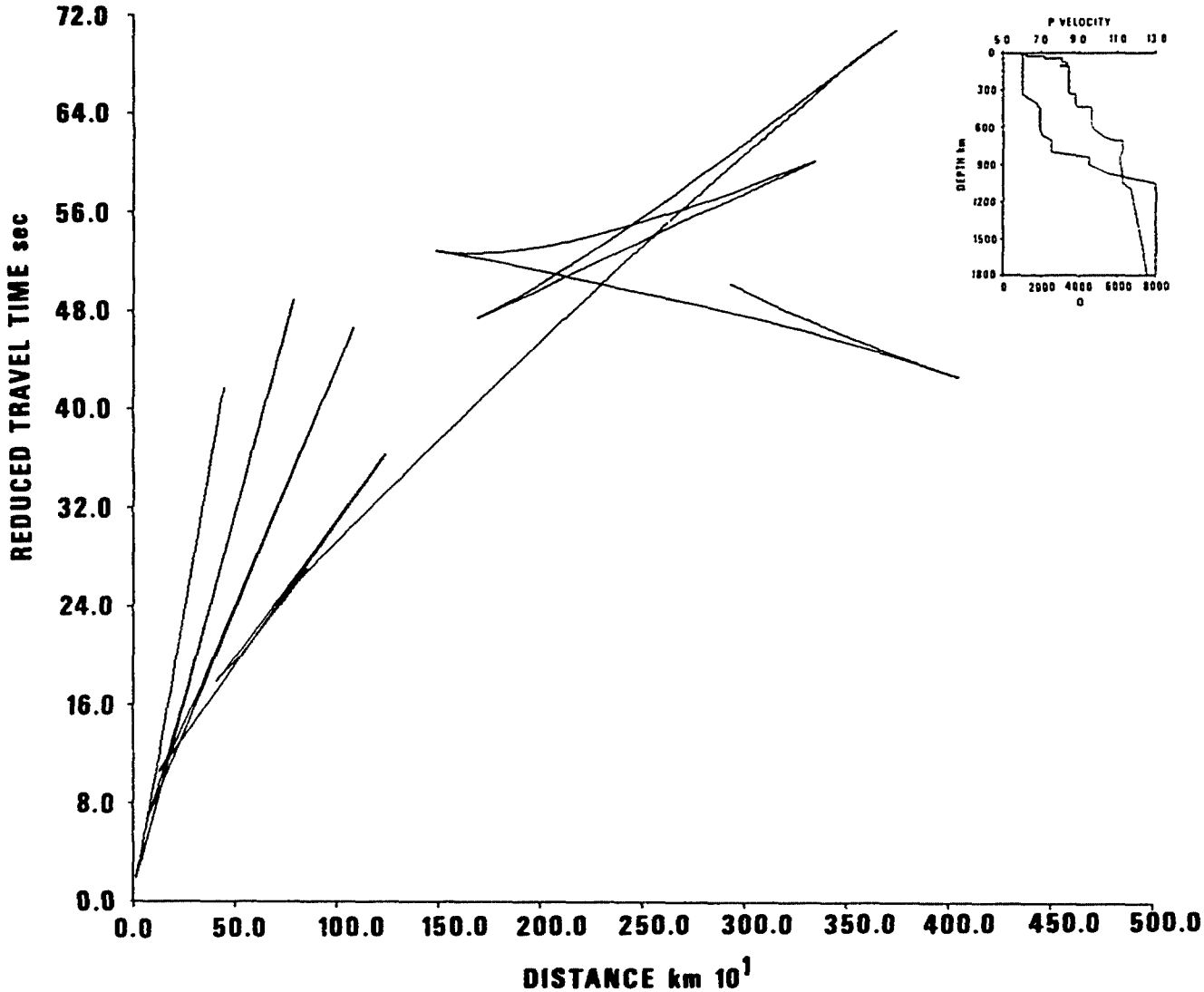

Figure 4a. Travel times for Massé's Eastern United States model with high Q values in the upper mantle.

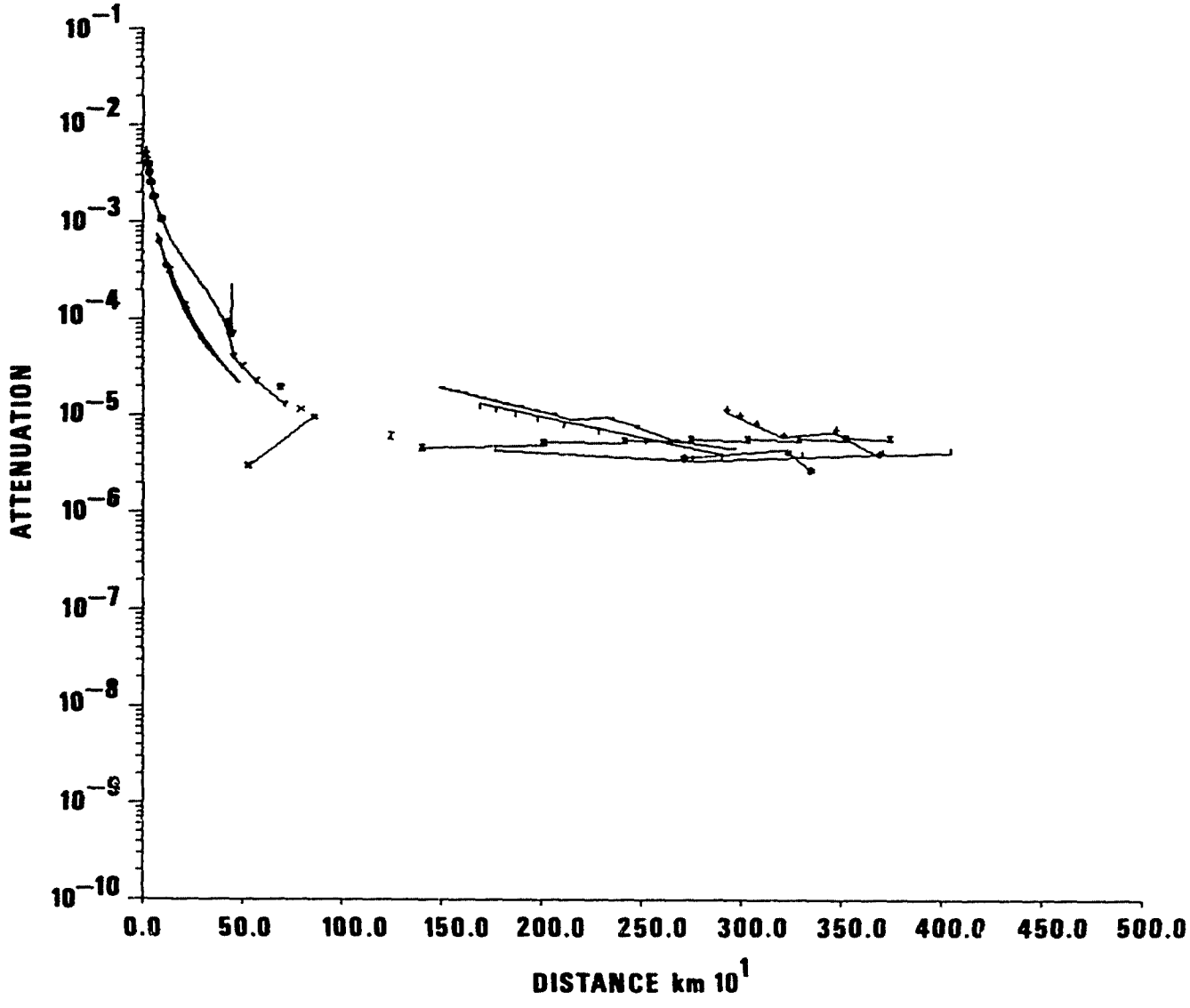

Figure 4b. Amplitudes for Massé's Eastern United States model with high Q values in the upper mantle. Without attenuation.

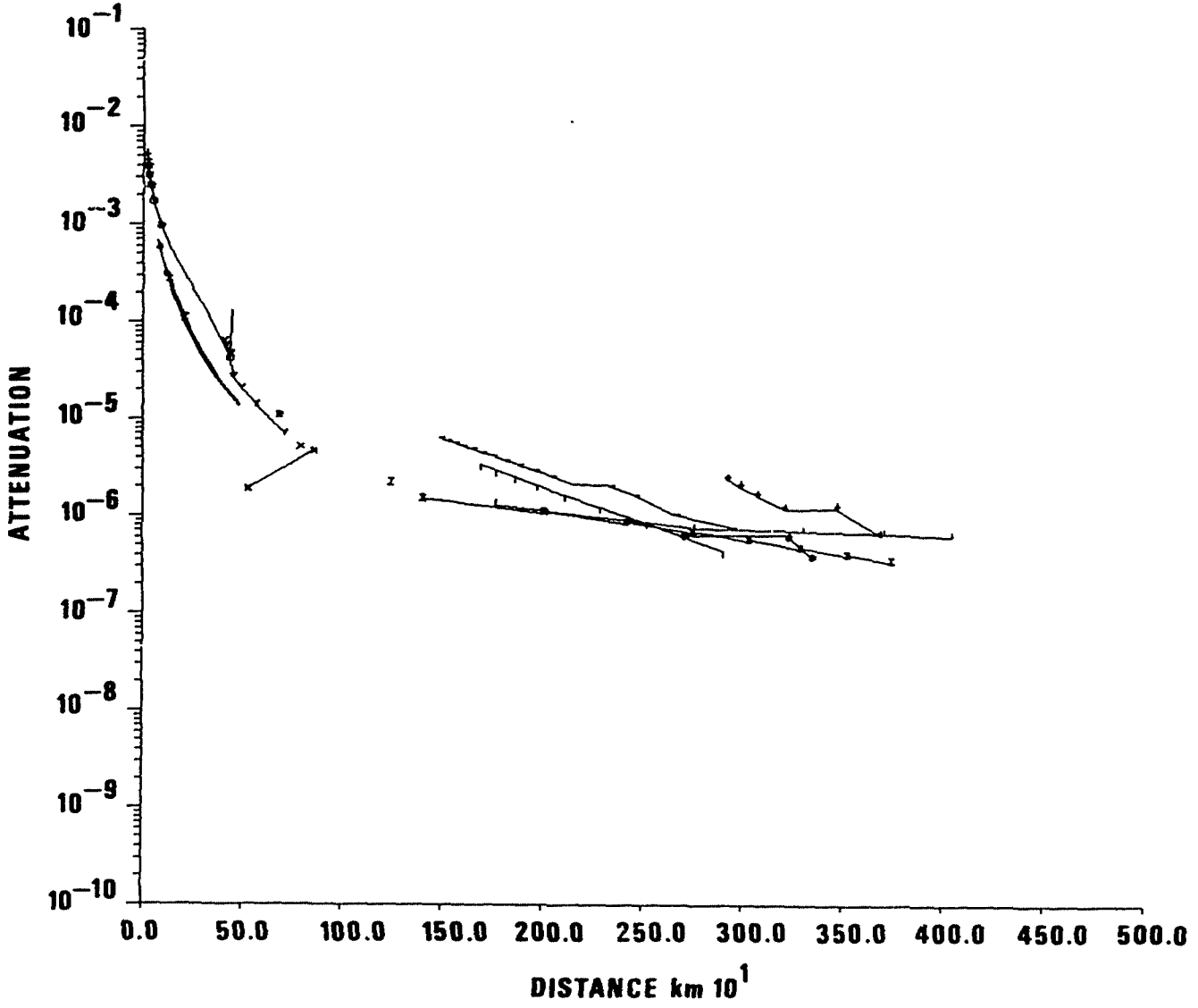

Figure 4c. Amplitudes for Massé's Eastern United States model with high Q values in the upper mantle. With attenuation at the period of T = .5 sec.

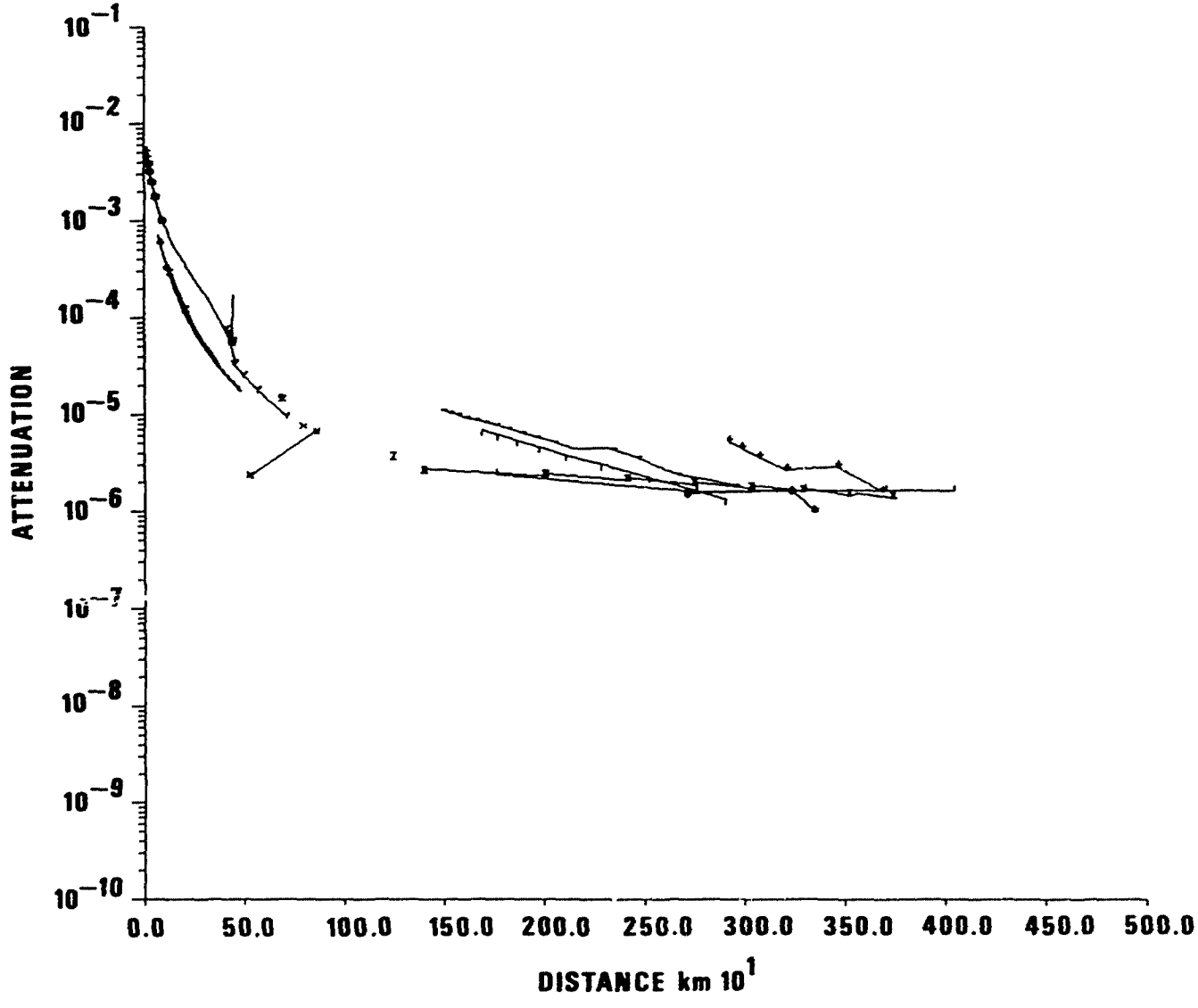

Figure 4d. Amplitudes for Massé's Eastern United States model with high Q values in the upper mantle. With attenuation at the period of T = 1 sec.

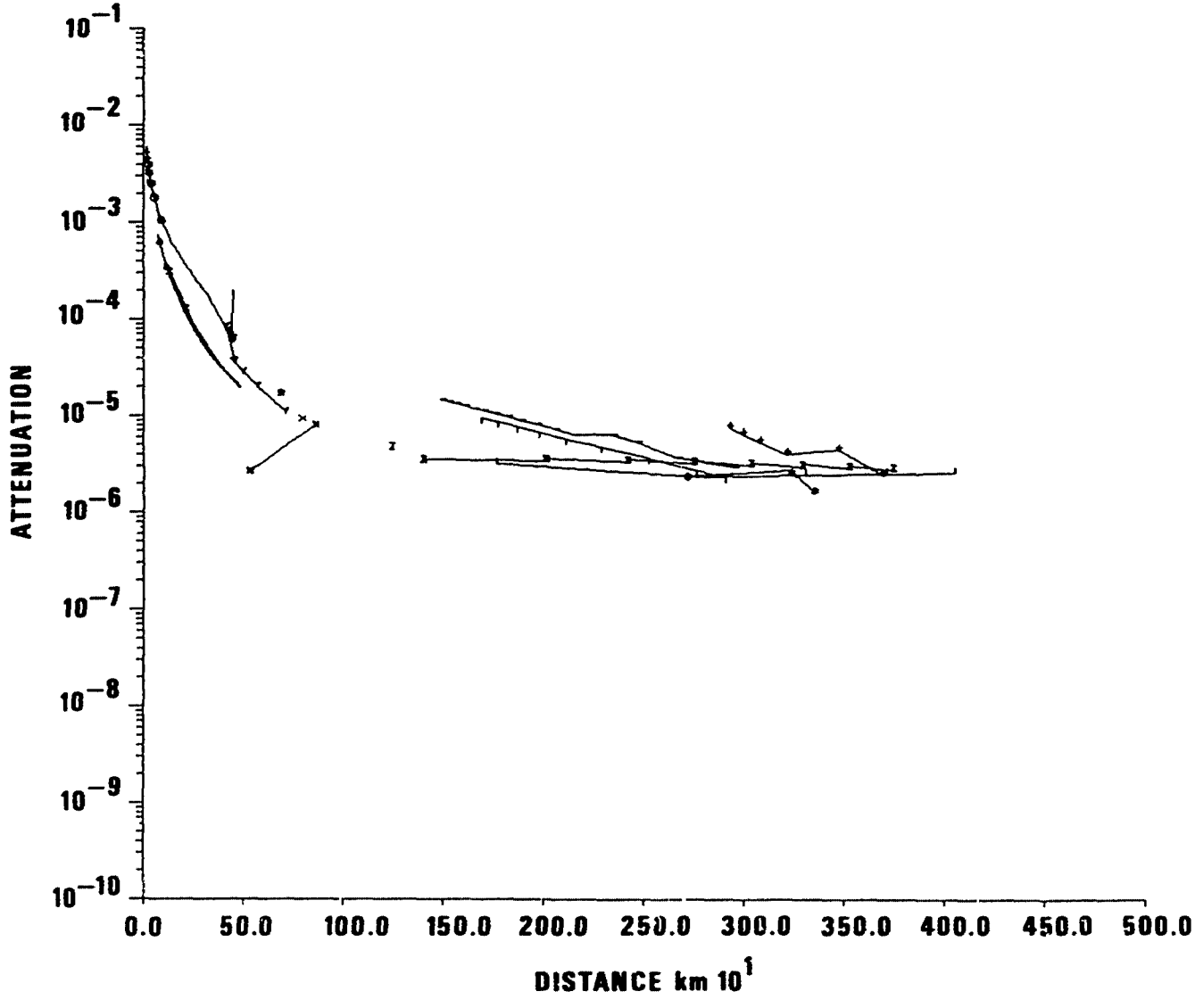

Figure 4e. Amplitudes for Massé Eastern United States model with high Q values in the upper mantle. With attenuation at the period of T = 2 sec.

falls off less sharply as the waves penetrate the corresponding portions of the mantle and the spectra of the various arrivals remain more similar to the source spectrum.

In the following discussions we shall emphasize results at stations beyond 1400 km from SALMON, since spectra of waves at these distances will be mostly influenced by the presence or absence of low Q layer and regional complications due to different velocity structures are less likely.

One should be able to estimate the average value of Q along the least time path from the source to a station by taking the spectral ratio of the early part of the P wave train to that of the source spectrum. A time window taken at the early part of the wave train may contain several arrivals along the various travel time branches. These multiple arrivals distort the spectrum, but they are unlikely to restore uniformly the high frequencies lost by attenuation. The resulting spectral ratios may not be well behaved, but they must reflect the loss at the high frequencies. The Q values derived from teleseismic-to-source spectral ratios will be crude, but they should be reasonably close to the real average Q along the path.

Local crustal effects at the station site also distort the spectra of body waves; however, as pointed out by Kanamori (1967a,b), they are more likely to introduce scalloping of the spectra than to produce a general decrease of amplitudes with frequency.

The effects of crustal response and multiple arrivals on the spectral ratios are more serious at small epicentral distances on high Q crust-mantle structures, where such factors can make the fluctuations of the small spectral slopes caused by attenuation as large as the slope itself. Nevertheless, although the Q values derived from such measurements can be unreasonably high, it is still possible to determine whether the paths in question cross low or high Q regions.

Kanamori, H., 1967a, Spectrum of P and PcP in relation to the mantle-core boundary and attenuation in the mantle, J. Geophys. Res., v. 72, p. 559-571.

Kanamori, H., 1967b, Spectrum of short-period core phases in relation to the attenuation in the mantle, J. Geophys. Res., v. 72, p. 2182-2186.

DATA ANALYSIS

SALMON, an underground nuclear explosion in a salt dome in Southern Mississippi, was well recorded at a large number of LRSM stations in the United States and Canada. P-wave portions of short-period vertical seismograms, also including a noise sample prior to the arrival of the P wave, were anti-alias filtered and digitized from magnetic tape at 20 samples/sec at selected LRSM stations along three profiles previously analyzed by Archambeau, Flinn and Lambert (1966). The location of stations used in the analysis are given in Figure 5.

Seismograms of these P waves are shown in Figure 6, grouped according to profile. As the N. W. profile crosses over the Rocky Mountain front, the dominant period of P waves increases to about 1 sec, while those with paths located entirely in Eastern North America have dominant periods around .3 to .5 sec.

A time window comprising 9 sec of the signal and 4 sec of the preceding noise was tapered with a Parzen window and Fourier transformed, and the power spectrum was computed by multiplying the Fourier spectrum by its conjugate. The resulting power spectrum was then smoothed by a 12-point running average. The shift of the time window was designed to avoid heavy tapering of the first arrival. A noise power spectrum ahead of this window was computed using an identical treatment. This noise spectrum was subsequently subtracted from the spectrum of the window containing the signal.

At the site of the explosion the near-field motion was measured by Patterson (1966) and Springer (1966). These close-in field measurements indicate that the source was very symmetrical azimuthally due probably to the plasticity of salt. The reduced displacement potential time functions $\psi(t)$

Archambeau, C. B., Flinn, E. A., and Lambert, D. G., 1966, Detection, analysis and interpretation of teleseismic signals, 1. Compressional waves from the SALMON event, J. Geophys. Res., v. 73, p. 3877-3883.

Patterson, D. W., 1966, Nuclear decoupling, full and partial, J. Geophys. Res. v. 71, p. 3427-3436.

Springer, D. L., 1966, Calculation of first zone P wave amplitudes for SALMON event and for decoupled sources, J. Geophys. Res., v. 71, p. 3459-3467.

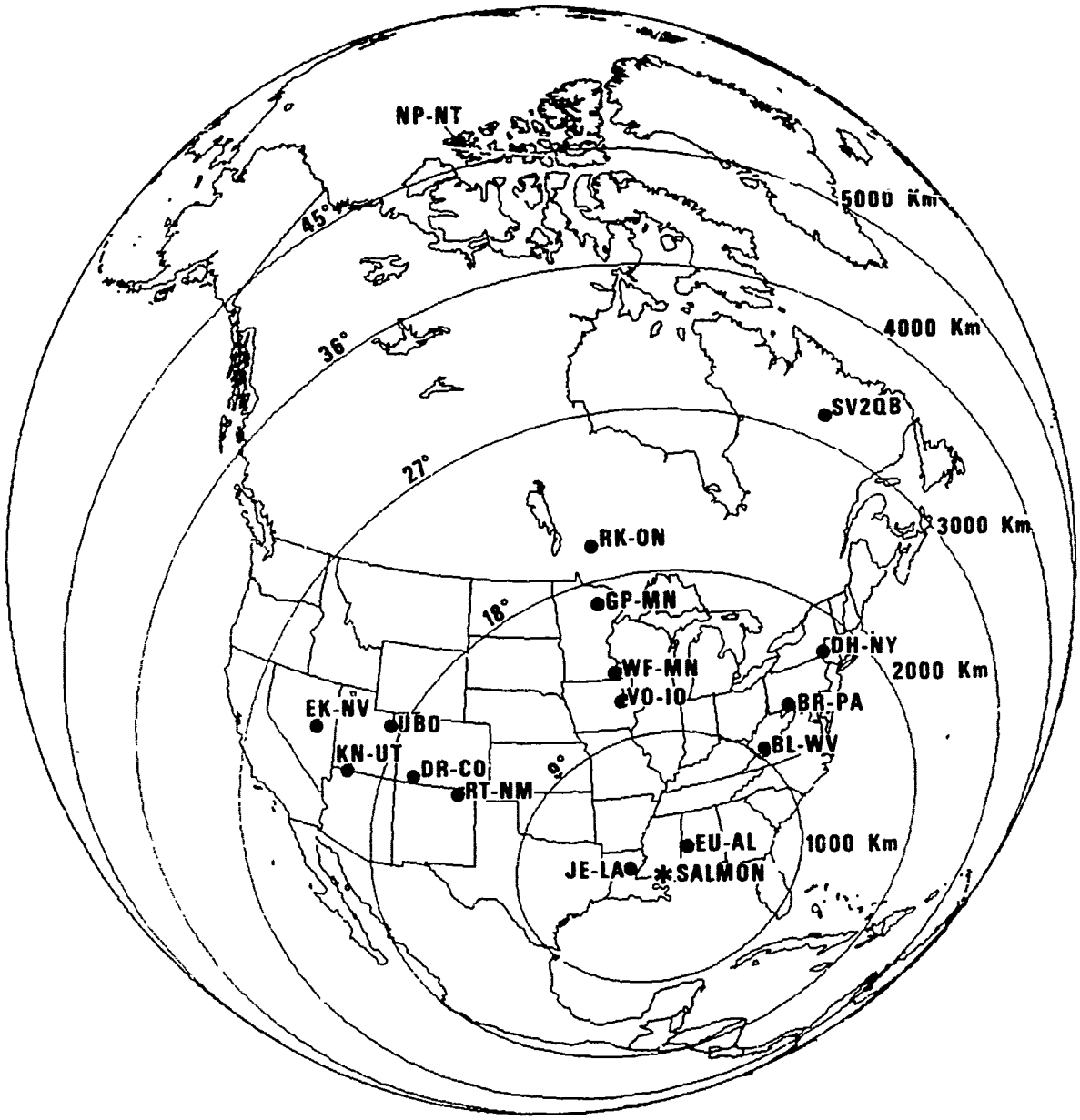

Figure 5. Location of SALMON and the stations used in the study.

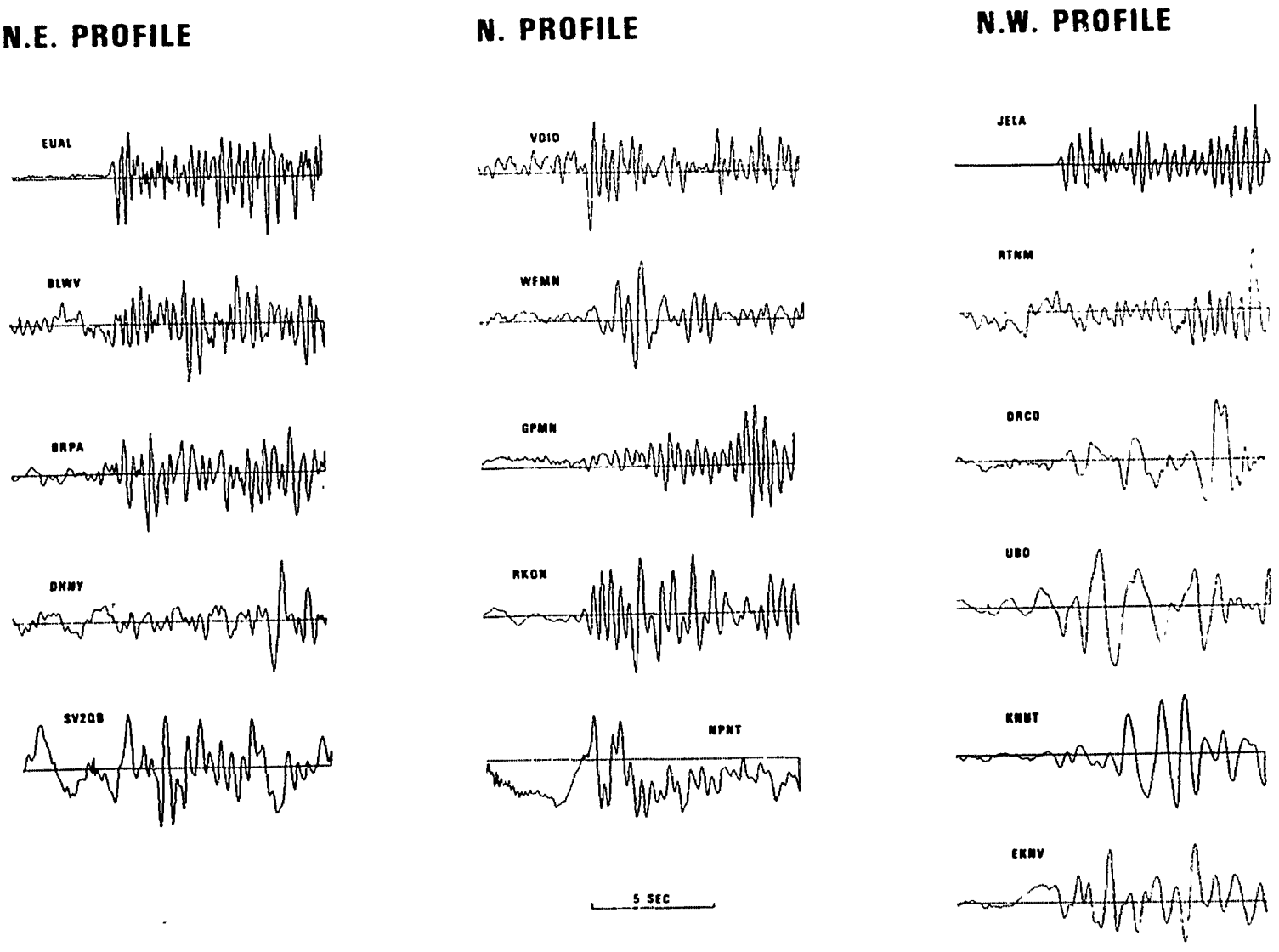

Figure 6. P wave seismograms used.

were derived from accelerometer gage records. These time functions, given by Patterson (1966) and shown in our Figure 7a, are used in this paper to derive estimates of the teleseismic displacement spectra. On the average these time functions rise to a maximum in .15 sec and have an overshoot of the order of 1.1-1.2 relative to the asymptotic value approached after .35 seconds. We have fitted von Seggern and Blandford's (1972) source time function model

$$\psi(t) \sim 1 - e^{-kt} [1 + kt - B(kt)^2]$$

where k and B are parameters to be fitted to observed time functions to approximate the average of the time functions given by Patterson. The parameters finally arrived at are k = 20, B = 1. The corresponding time function shown in Figure 7b is similar to those shown in Figure 7a, but it rises steadily instead of having an inflection point at the beginning. The power spectra were subsequently computed by the formula given by von Seggern and Blandford (1972).

$$u(\omega) \sim \frac{[A'^2(\omega/k)^2 + 1]^{1/2}}{[(\omega/k) + 1]^{3/2}}$$

where $A' = 2B+1$. This formula gives a falloff at the rate of ω^{-2} in the teleseismic amplitude spectrum, which agrees with the observations better than the ω^{-4} rate predicted by Haskell's (1967) source theory.

Another source power spectral estimate was directly obtained from the potential function shown in Figure 7c which is an average of all the time functions given by Patterson. This waveform was differentiated numerically and its Fourier transform was squared to obtain another estimate of the source spectrum.

As a third reference we used the spectrum at EUAL. All three spectra (EUAL spectrum corrected for instrument response) are shown in Figure 8.

We consider the spectrum derived from the differentiated average displacement potential waveform to be the most realistic, since it was derived

---

von Seggern, D. and Blandford, R., 1972, Source time functions and spectra for underground nuclear explosions, Geophys. J. R. A. S., v. 31, p. 83-97.

Haskell, N. A., 1967, Analytic approximation for the elastic radiation from a contained nuclear explosion, J. Geophys. Res., v. 72, p. 2583.

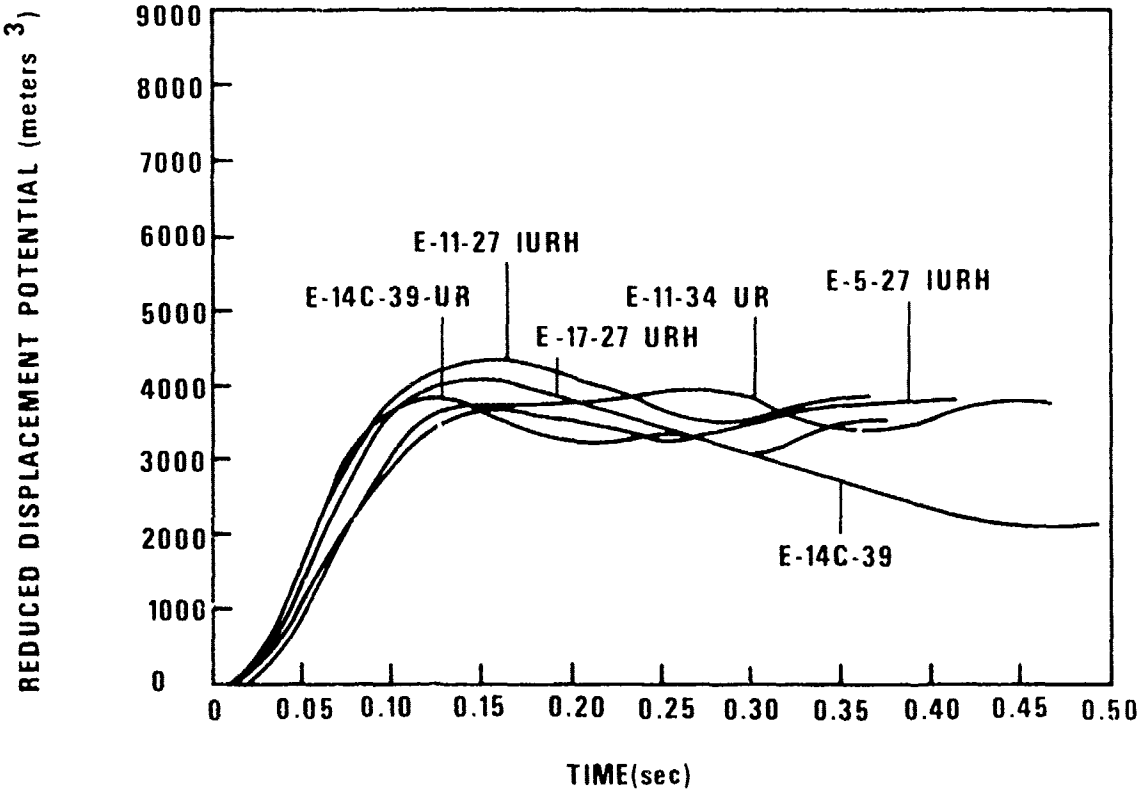

Figure 7a. Reduced displacement potentials for SALMON as given by Patterson at various close-in observing stations.

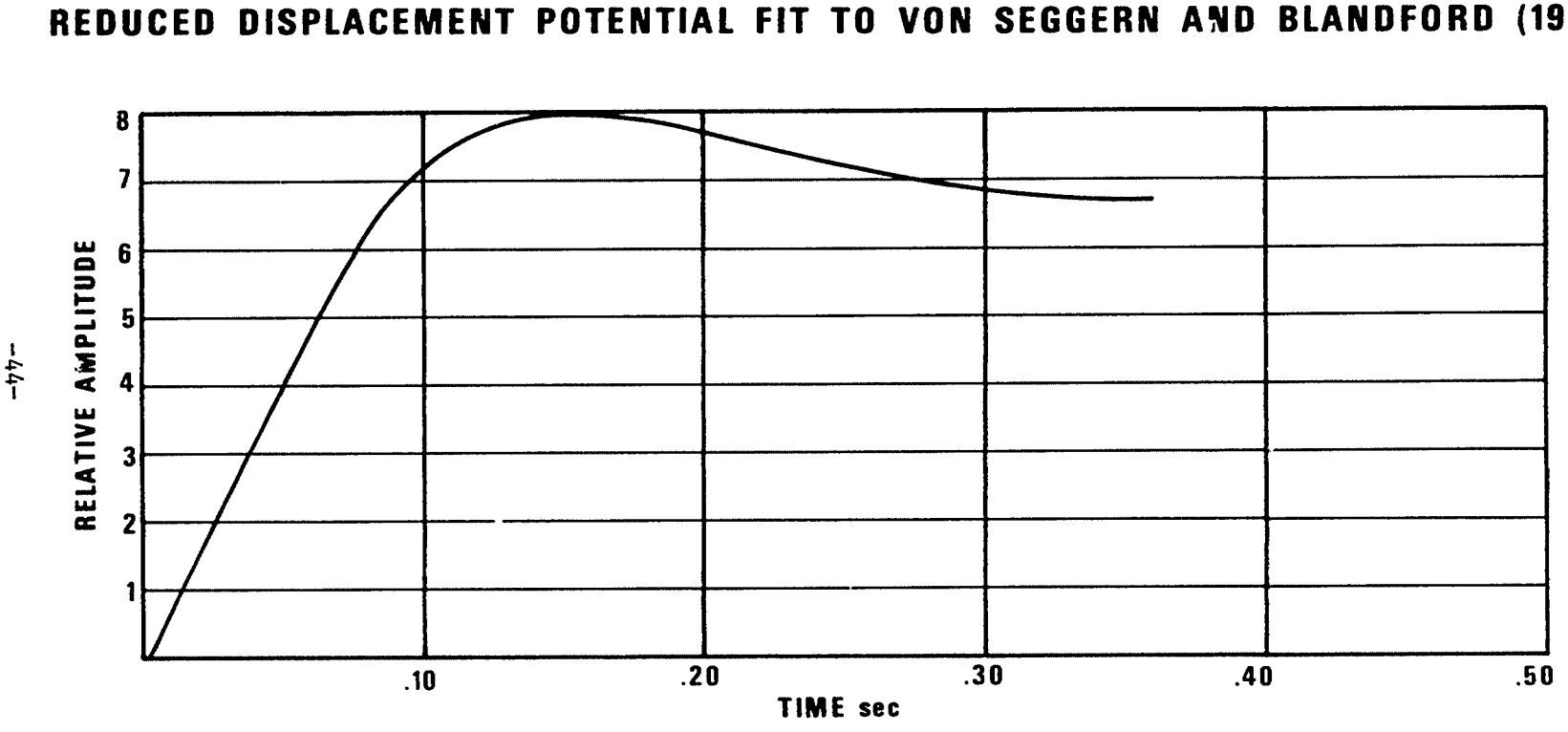

Figure 7b. Reduced displacement potential as derived from the theory of von Seggern and Blandford.

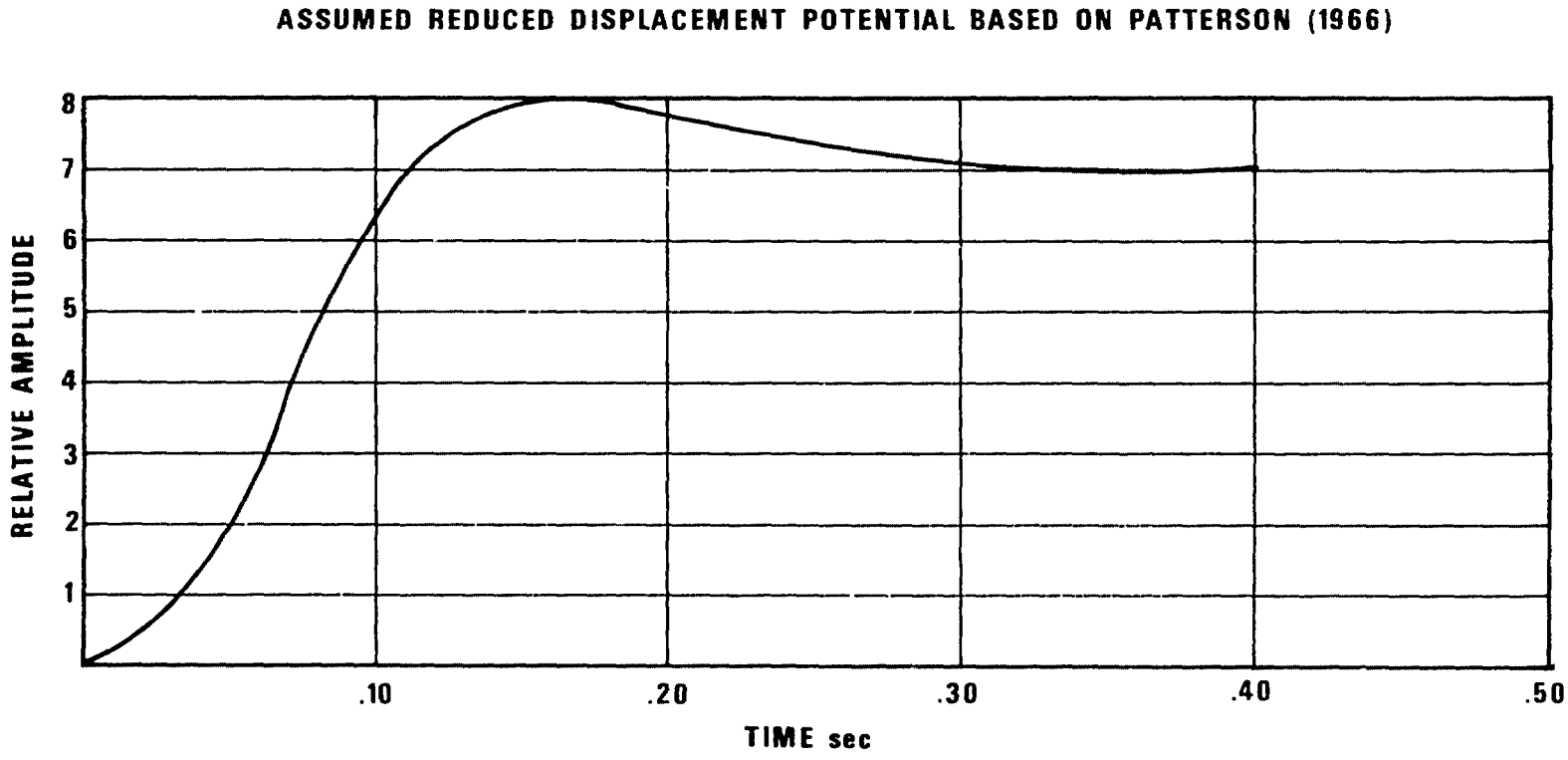

Figure 7c. Reduced displacement potential used to derive close-in source spectrum.

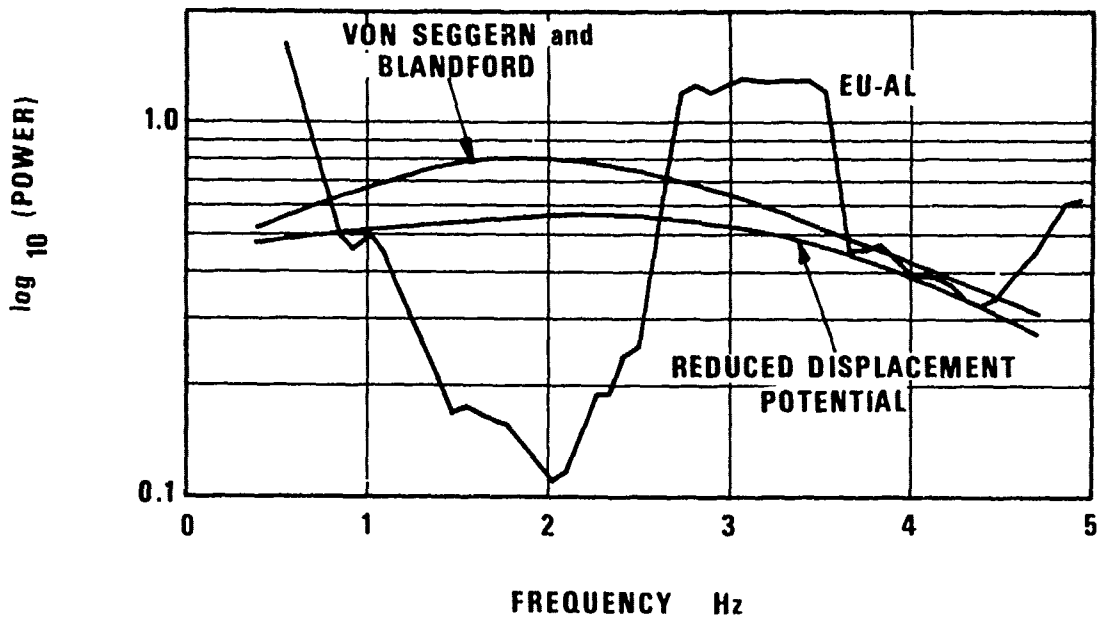

Figure 8. Reference source power spectra used in this report.

from measurements in the most direct manner. The source power spectra were modified using the LRSM instrument response and smoothed with a 12-point running average. This was done to simulate an identical treatment given to the data spectra (the effect of the Parzen window is not very significant relative to the 12-point smoothing).

Before computing spectral ratios, one has to consider and correct for the effect of the surface reflection above the source. Near-field measurements give a vertical uphole time of .27 seconds which implies a pP-P time interval of about .47 seconds assuming a takeoff angle of about 30 degrees from the vertical to most of the stations analyzed. However, inspection of most unsmoothed spectra did not reveal any clear modulation which could be associated with such a pP-P travel time difference. The curved upper surface of the salt dome might account for this. A few spectra show modulation which might be interpreted as pP, but even in those cases alternative sources of modulation such as crustal response or multipathing are possible. Thus, even if a pP phase is present it might be weak or obscured by other effects. For this reason instead of "correcting" the spectra for pP, which for any sizeable surface reflection coefficient would introduce spurious peaks into the spectrum, we rely on smoothing to eliminate any modulation present due either to pP or to other causes. We shall fit straight lines to spectral ratios and this will constitute, in effect, a final smoothing. Even the null at zero frequency might be eliminated by a curved saltdome-sediment interface. In any event, since we do not use frequencies below .5 Hz and because our straight line fits to the spectral ratios use frequencies up to 4 Hz, the effect of any such null on the slopes is minimal.

In order to insure reasonable data quality, we took a noise sample prior to the arrival of the signal, and in fitting straight lines to the spectral ratios we required that the signal power spectrum exceed that of the noise by a factor of three. Furthermore, in order to avoid problems with the dynamic range of analog magnetic tapes, the portions of power spectra which were down more than 2.5 orders of magnitude from the peak were also disregarded. These conditions eliminated some stations, such as HNME and LSNH, which were favorably located, but showed high levels of microseismic noise. The 3:1 ratio condition for power spectra was relaxed for the station SV2QB; it is 2:1 there. The slope obtained therefore is less reliable. It is

significant, though, that the spectral peak is at 2 cps indicating that attenuation is relatively low along the path to this station.

The spectra computed for each station are shown in Figure 9. Again, the spectra of the western stations show low relative amplitudes at the higher frequencies. Stations close to the source should have spectra similar to the source spectrum. The source spectrum and those of EUAL and JELA, the closest stations, are indeed similar, but the JELA spectrum shows a sharp peak not present in the EUAL or source spectrum. Amplitudes at JELA are also anomalous (Springer, 1966) which may indicate that this station is located on sediments causing local resonance effects which distort the spectrum. JELA is, in fact, located in a sedimentary basin on sandstone, and EUAL is in mixed sand and clay. Spectra at both sites might, therefore, be suspect.

To obtain Q values we have computed spectral ratios of the individual spectra to all three selected reference spectra. The spectral ratios and the least squares straight line fits are shown in Figure 10 for the EUAL source spectrum, Figure 11 for source power reduced spectrum of von Seggern and Blandford, and Figure 12 for the source spectrum derived directly from the observed displacement potential. The travel times, distances, approximate first arrival penetration depths, slopes of $\log_{10}$ spectral ratios versus frequency, and average Q values are given in Table II for the three reference spectra mentioned. The ratios for all reference spectra are similar. Very small slopes at some close-in stations may indicate that some of the reference spectra used are deficient at higher frequencies. Assuming that the average Q to EUAL is about 1000, the travel time is about 36 seconds which should result in a slope of about .04 in the $\log_{10}$ (Ratio) - frequency plane. Correcting for this effect would not result in any significant changes in the conclusions of this report.

The Q values derived from all three reference spectra are higher in the eastern U. S. than in the western U. S. The unrealistically high and even negative Q values for some eastern U. S. stations imply that the standard deviation of the slope estimate is greater than the slope itself. It can, however, be said that Q must be well over 1000 for all eastern paths with the exception of WFMN. We have found no obvious explanation for the low Q

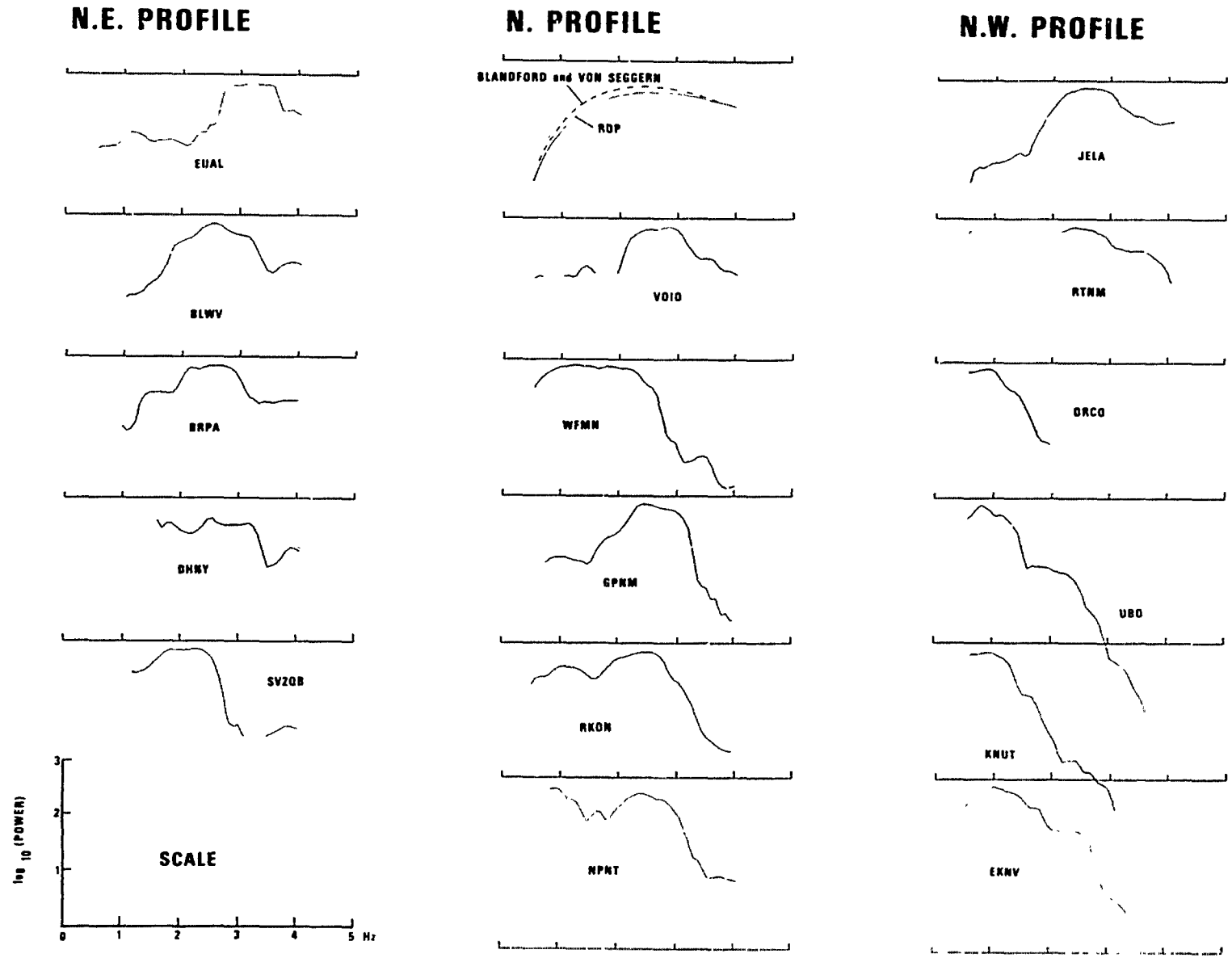

Figure 9. Power spectra of P waves at various observing stations. The theoretical source spectra used in the calculations are shown in the upper middle of the figure.

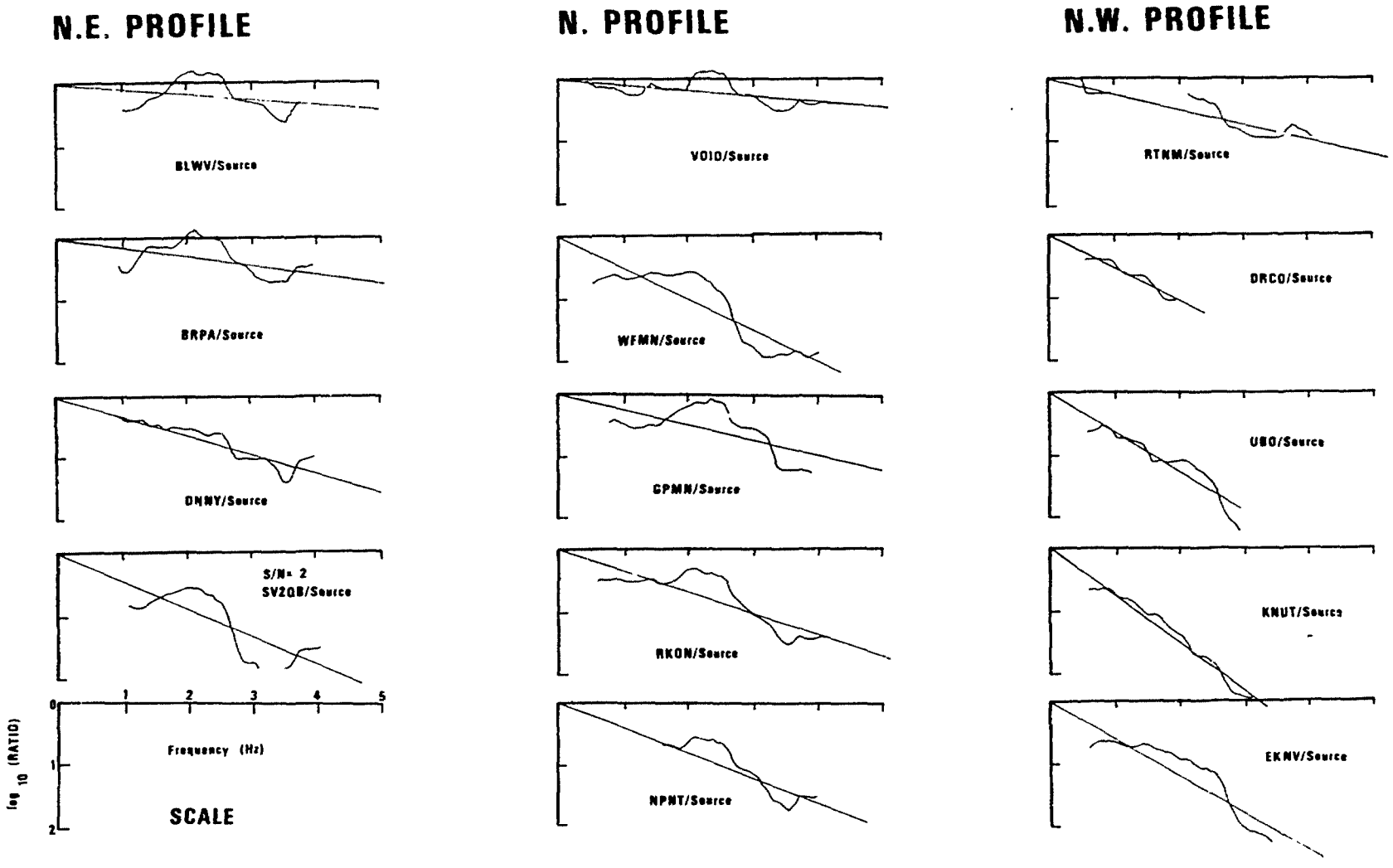

Figure 10. Ratios of P-wave amplitude spectra at the individual stations to the amplitude spectrum at EUAL.

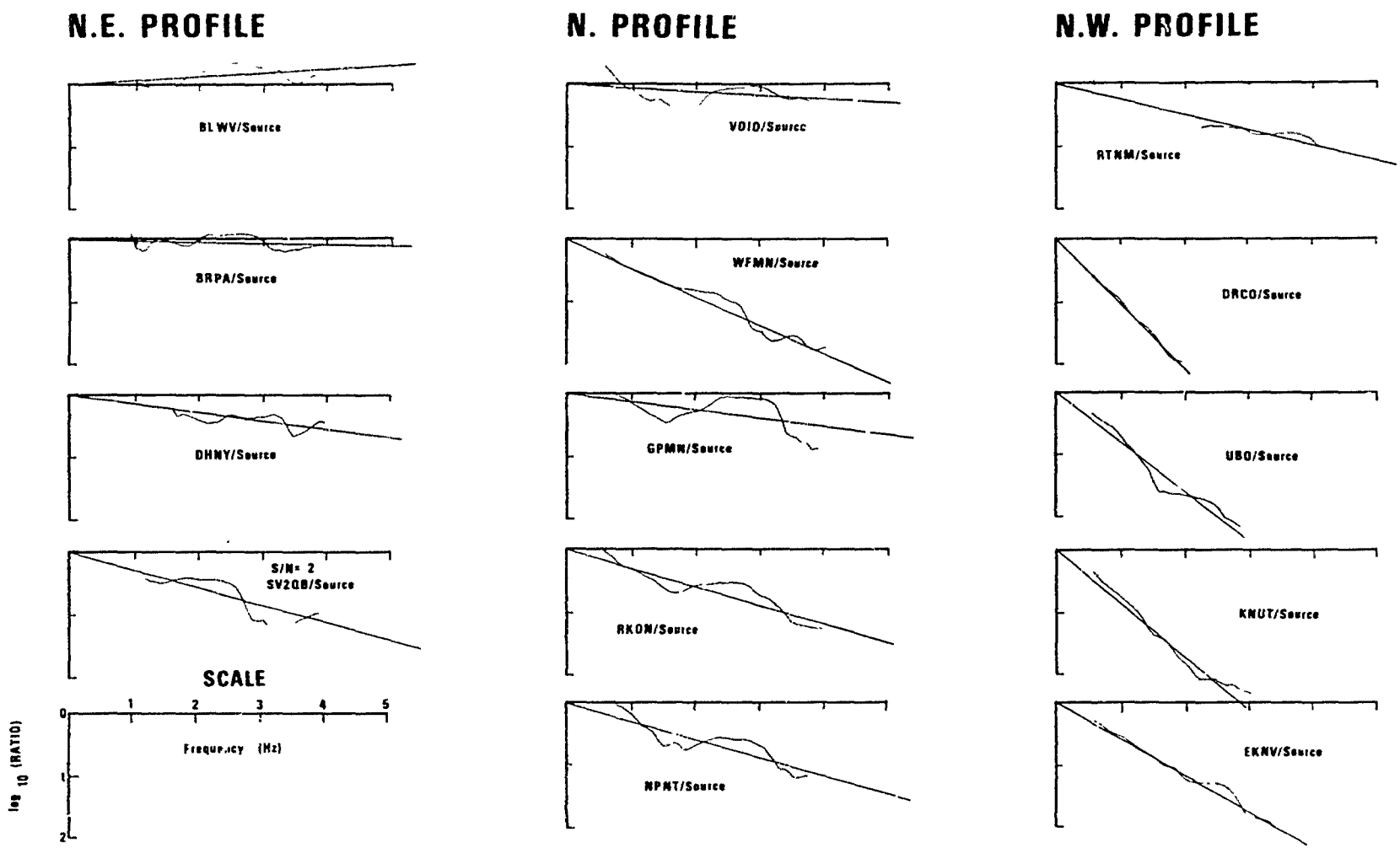

Figure 11. Ratios of P-wave amplitude spectra at the individual stations to the source spectrum derived from the formula of von Seggern and Blandford.

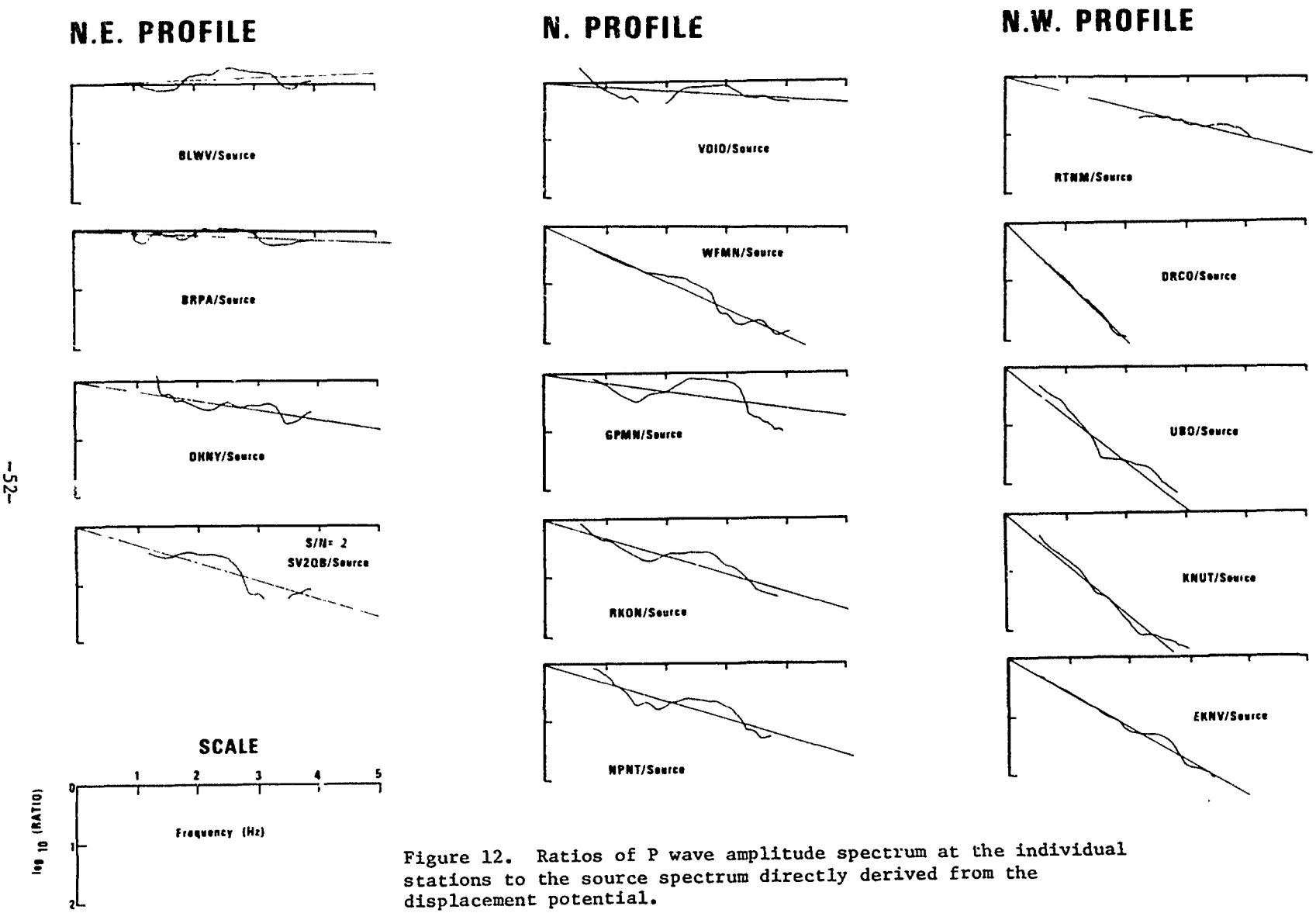

Figure 12. Ratios of P wave amplitude spectrum at the individual stations to the source spectrum directly derived from the displacement potential.

TABLE II

Travel times, slopes of amplitude spectral ratios average Q values and approximate penetration depths for various stations

Station	Geology	Distance (km)	Travel Time Min	Sec	Approx. Depth of Penetration (km)	Ref: EUAL Slope	Ref: EUAL Q	Ref: Source (von Seggern & Blandford) Slope	Ref: Source (von Seggern & Blandford) Q	Ref: Source Displ. Potential Slope	Ref: Source Displ. Potential Q
	N. E. Profile										
EUAL	Clay and Sand	242	0	36.5	30?	-	-	.042	∞	.025	∞
BLWV	Sandstone	1058	2	16.5	110	-.085	2223	.058	∞	.036	∞
BRPA	Sandstone	1375	2	54.0	120	-.139	1708	- .018	13189	- .039	6087
DHNY	Sandstone	1795	3	45.3	440	-.307	1001	- .146	2105	- .168	1830
SV2QB	Metamorphic	3192	5	58.0	>600						
	N. Profile										
VOIO	Limestone	1251	2	40.6	120	-.086	2548	- .060	3652	- .076	2883
WFMN	Limestone	1427	3	00.0	120	-.503	488	- .461	533	- .477	515
GPMN	Thin glacial drift over pre-cambrian	1865	3	51.4	400	-.236	1338	- .131	2410	- .151	2091
RKON	Granite	2214	4	30.5	430	-.341	1082	- .300	1230	- .316	1168
NPNT	Alluvium	5264	8	35.0	>600	-.397	1770	- .299	2350	- .319	2205
	N. W. Profile										
JELA	Sandstone	243	0	37.4	30?	.013	∞	.055	∞	.038	∞
RTNH	Limestone	1499	3	10.0	120	-.251	1033	- .253	1025	- .268	967
DRCO	Granite	1814	3	50.7	400	-.554	568	-1.059	297	-1.048	300
UBO	Sandstone	2069	4	20.1	400	-.633	561	- .804	441	- .808	439
KNUT	Sandstone	2234	4	37.3	430	-.776	488	- .863	438	- .871	434
LKNV	Shale	2533	5	05.4	460	-.606	688	- .592	704	- .604	690

measurement for the station WFMN; however, the spectrum at this station falls off sharply at 2.5 Hz, which contributes considerably to the large slope. If we fitted the slope only up to 2.5 Hz, the result would be much less. The western stations have the ascending portion of the raypath in crust-upper mantle velocity and Q structure appropriate to the western U. S. with the exception of RTNM which lies at the edge of the boundary (Der, Massé, and Gurski, 1975; Booth, Marshall, and Young, 1975). Correspondingly, all western stations except RTNM show lower Q's than eastern stations (WFMN excepted).

The penetration depths were computed from Massé's (1973) model for the eastern United States. Depending on what kind of crust-upper mantle model one is willing to accept, these depths may vary somewhat. But all reasonable models are such that first arrival P waves at epicentral distances beyond 1700-1800 km must penetrate to great depths in the upper mantle (of the order of >400 km), while at epicentral distances up to 1400 km the penetration depth of some raypaths may be shallow for some structures, with the waves still remaining in the lithosphere above the lid of the low velocity layer (if it exists). Since we are primarily interested in the condition of the upper mantle, the stations with great P wave penetration depth are of primary interest. Paths to the western stations go through two basically different velocity structures, but since the first half of the paths are under the eastern United States, the penetration depths are primarily determined by the structure in the East. Gradual changes from one structure to the other, proposed by some investigators (Green and Hales, 1968; Yasar and Nuttli, 1974), would also modify the raypath somewhat, but the depths of penetration would not change much.

Massé, R. P., 1973, Compressional velocity distribution beneath central and eastern North America, Bull. Seism. Soc. Am., v. 63, p. 911-935.

Green, R. W. E. and Hales, A. L., 1968, The travel times of P waves to 30° in the central United States and upper mantle structure, Bull. Seism. Soc. Am., v. 58, p. 267-290.

Yasar, T. and Nuttli, O. W., 1974, Structure of the shear-wave low-velocity channel in the western United States, Geophys. J. R. A. S., v. 37, p. 353-364.

DISCUSSION

In order to evaluate differences between paths which remain in the stable eastern part of the United States (EUS) and those which cross over into the western United States (WUS), we consider only seven stations for which the penetration depths is of the order of 400 km. To simplify matters we assume vertically homogeneous but different upper mantles for both the eastern and western United States (as in Berzon et al., 1974). The attenuation coefficients then can be written as

$$\alpha = \frac{\pi \cdot T}{Q_{av}} = \bar{\alpha} T$$

where T is the wave travel time and Q_{av} is the average Q in the upper mantle. We then average the values of $\bar{\alpha}$ for each region. The values of $\bar{\alpha}$ for each station and their averages using the source spectrum derived from the reduced displacement potential are given in Table III. We compute a typical difference in amplitudes for a 1 cps wave which travels for 4.0 minutes (to a distance of approximately 1800 km) in a typical eastern U. S. structure vs. a mixed path. This amounts to .56 magnitude unit. The same size magnitude difference was indeed observed for SALMON as the rays crossed the Rocky Mountain front (Jordan et al., 1966). Thus spectral ratios, relative measurements, seem to predict correctly the differences in the magnitudes of the western stations relative to those in the eastern part of the continent.

Consider again the seven stations which we divided between those with entirely eastern paths and those with mixed paths. Averages of the values of $\bar{\alpha}$ require a Q_{av} of 1588 for eastern paths and 427 for mixed paths for the stations chosen. The value 1588 is lower than the average Q of all eastern stations. Q in the east can be even higher as indicated by Q values along paths differing in penetration depths from those used in Table III. Assuming that the mixed paths are evenly divided between the eastern and

---

Jordan, J. N., Mickey, W. V., Helterbran, W., and Clark, D. M., 1966, Travel times and amplitudes from the SALMON explosion, J. Geophys. Res., v. 71, p. 3469-3482.

TABLE III

Calculation of the relative attenuation along paths in the EUS structure relative to mixed paths

	$\bar{\alpha} \times 10^5$		$\bar{\alpha} \times 10^5$
DHNY	74.6	DRCO	454.3
GPMN	65.8	KNUT	314.1
RKON	116.8	EKNV	197.8
avg. $\bar{Q}_E$	85.7	UBO	310.7
		avg. $\bar{Q}_M$	319.2

The relative amplitude factor D with 4 minutes travel time becomes for 1 cps waves

$$D = \exp[(319-86) \times \ln 10 \times 10^5 \times 240] =$$

$$= \exp(1.27) = 3.65$$

This corresponds to

$$\log_{10}(3.65) = .56 \text{ magnitude units.}$$

western United States, which is roughly true, Q_{av} must be about 246 along the ascending part of the wavepath. We shall use the round figures 1600 and 250 for average Q along paths in the EUS vs WUS in the following instead of 1588 and 246 derived above.

The attenuation of waves which travel along teleseismic paths cannot be derived uniquely from our results without making assumptions about the vertical structure of the low Q zone and the Q values in the lower mantle. If the Q in the upper mantle between the base of the crust and 400 km depth were constant, the time spent in this zone by waves travelling along teleseismic paths would be considerably less than that along the four paths used for calculation of Q in the west. In this case our results could explain a magnitude difference of only .23 magnitude units by attenuation, since at near vertical incidence the travel time through the upper 400 km of the mantle is only about 50 seconds.

The assumption of constant Q over such a depth range is, however, unrealistic. Surface wave inversion and the results of Archambeau et al. (1969) indicate that the low Q zone in the earth bottoms at around 200 km depth. If so, the difference between the travel times of teleseismic paths and the paths used in this study would not be very great, and our results would then be consistent with, and completely account for, the .3-.4 magnitude unit differences between teleseismic magnitudes measured in the eastern vs western United States (Booth et al. 1975).

If the lowest Q values are concentrated above 200 km depth, the average Q of the upper 400 km of the earth at vertical incidence will be less than 250. Since paths of teleseismic waves and the paths used in this study spend roughly the same time in the upper 200 km of the mantle, any vertical Q distribution in this depth range, which at near vertical incidence yields an average teleseismic Q between 150-200 in the western United States vs 1600 for the eastern part of the continent, will be consistent with the .3-.4 magnitude difference of teleseismic magnitudes found by Booth et al. and many other investigators. These Q values may seem low, but if all attenuation found along the ascending path from SALMON is concentrated in the uppermost part of the mantle, a layer a few tenths of kilometers thick

just below the Moho for instance, a vertical Q average as low as 104 results. This is obviously another extreme condition as unlikely as is the assumption of a constant Q spread out over 400 km.

The above values are considerably lower than those of Archambeau et al. (1969), whose model yields an average Q of 375 for the upper 400 km of the upper mantle at vertical incidence. It is possible, though, that some of the ascending wavepaths used in their analysis were outside the region underlain by the low Q layer, thus biasing the results toward higher Q's. Thin, low Q layers were found by Veith and Clawson (1972) using mostly data from NTS explosions. Their NTS model has a layer about 100 km thick with a Q of 110 underlain by a region with a constant Q of 500. The average Q at vertical incidence in around 290 in this structure for the uppermost 400 km section. Another model also derived by Veith and Clawson using Herrin's velocity model has a rough vertical average Q of only 200 over the same depth range. These results are consistent with ours.

Frasier and Filson (1972) and Noponen (1975) measured Q from NTS to NORSAR and obtained values around 1700. At these distances most of the travel time is spent traversing the high Q lower mantle. The value of 1700 can be reconciled with our results if we assume Q values of the order of 3000 or higher in the lower mantle below 400 km, $Q_\alpha \sim 1600$ for the ascending upper part (with travel time of 50 seconds), and $Q_\alpha \sim 250$, a relatively high value for the 50 sec travel time segment under NTS. The total travel time being around 700 seconds thus yields

$$t^* = \frac{50}{250} + \frac{600}{3000} + \frac{50}{1600} = .2 + .2 + .03 = .43.$$

This value is close to $t^* = .42$ reported by Frazier and Filson (1972) and Noponen (1975), but it must be noted that this analysis is strongly influenced

---

Veith, K. F. and Clawson, G. E., Magnitude from short-period P wave data, Bull. Seism. Soc. Am., v. 62, p. 435-452.

Noponen, I., 1975, Compressional wave power spectrum from seismic sources, Institute of Seismology, University of Helsinki, ISBN 951-45-0538-7. Contract AFOSR-72-2377 Final Report.

by the assumed lower mantle Q's which are poorly known. Note that higher Q values in the deeper mantle can always be used to compensate for lower Q values in the upper mantle. At present, the uncertainties of lower mantle Q values preclude a more exact analysis.

Another result of Noponen is a Q value of 2000 or larger from Kazakh to NORSAR at an epicentral distance of about 30°. This is comparable to our results for the paths from SALMON to NPNT and SV2QB and is probably a representative value for paths under stable shield-type regions.

Trembly and Berg (1968) found average Q values of 450 from NTS to NPNT a distance of the order of 4000 km. This value seems low compared to our results since we have observed similar Q values at smaller distances, and at greater distances the wavepaths spend more time in the mantle below 400 km depth where the Q is presumably high, thus their Q should be higher. An average Q value of 450 along the mixed path NTS-NPNT would result in a magnitude differential relative to purely shield type (Eastern U. S. to NPNT with Q in the 1600-2000 range) paths of about 1 magnitude unit (at 1 cps), which is much too high compared to the .3-.4 magnitude unit differences observed by Booth et al. (1975).

The above considerations lead us to believe that the teleseismic magnitude differences between the eastern and western halves of the United States can be explained completely by anelastic attenuation. From our data at least .23 magntiude difference must be attributed to attenuation, but any vertical distribution of Q based on a wealth of geophysical data suggesting a low Q layer thinner than 400 km would yield differences of the order which can explain the magnitude difference fully by attenuation. Examination of the bedrock types in Table II reveals sandstone and granite in both east and west suggesting that crustal layering at the receiver can not be an explanation for observed differences between EUS and WUS. In trying to explain the differences in magnitudes by differences in crustal structures, one should find a crustal structure which decreases the amplitudes of <u>both</u> P and S waves (Der et al., 1975) while at the same time imposing the type of spectral differences observed by many workers for both types of waves over a wide period range (at least 0.3 to 4.0 seconds). Even leaving aside the evidence of stations on similar bedrock in EUS and WUS, we are not aware of a structure which could meet these requirements.

COMMENTS AND CONCLUSIONS

The results reported here indicate that most or all of the difference in teleseismic magnitude values between eastern and western North America can be explained by anelastic attenuation in the upper mantle under western North America. The results indicate that under the stable eastern portion of the United States the Q for P waves is 1600, at least to the depth of 400 km. The western United States, on the other hand, is characterized by a low Q ($\leq$ 250 for vertical incidence) region located in the same depth range within the upper mantle. This seems to correlate well with many velocity studies which indicate that a P-wave low velocity layer is present under the western United States. Our western Q value may seem low, but Q_α values as low as 50 and Q_β values of 20 can occur in the earth and have been found behind some island arcs (Barazangi, Pennington and Isacks, 1975).

As a consequence of low Q values in the upper mantle, explosions in the western United States will seem to release less energy at teleseismic distances than events of same size on shields since attenuation under the sources will reduce the amplitudes of body waves. The same may be true for sources located in other tectonic regions with highly attenuating upper mantles. Sources with the same energy release in shield regions, on the other hand, should appear to release more energy due to the more efficient propagation under shields.

Since most U. S. nuclear explosions were located in the western United States, correction for attenuation is important if one is to establish a world-wide yield-magnitude scale based on these events.

Barazangi, M., Pennington, W., and Isacks, 1975, Global study of seismic wave attenuation in the upper mantle behind island arcs using pP waves, J. Geophys. Res., v. 80, p. 1079-1092.

The explosion SHOAL in granite for example was very near station SZNV, also on granite, which was operational from January 5 - February 8, 1963. This station lies about 1° North of MNNV within the triangle formed by MNNV, MVCL, and WINV, all of which have station corrections of -0.3 magnitude units. To check if the magnitude correction of SZNV was also -0.3, we measured corresponding cycles of corresponding signals at MNNV and SZNV for the first 20 events in the LRSM bulletin after January 5, 1963, having a reported amplitude at MNNV greater than 15 millimicrons. The mean magnitude difference and standard deviation of the mean (MN-SZ) was 0.04 ± 0.04. With 4 regional events removed the difference was -0.06 ± 0.04. The results are not significantly different from zero. Thus a station on granite near an underground explosion in granite has the same teleseismic residual as the average for western stations. This is likely to be the core for NTS too although there are no stations very close to NTS to rule out a window through which high frequencies can propagate to great distances.

ACKNOWLEDGMENTS

Mr. John Lambert assisted in the preparation of the data for this report. We thank Dr. Bruce Julian for making his raytracing program TVT2 available to us. Drs. Robert Blandford and Shelton Alexander contributed to this paper through useful advice and criticism.

REFERENCES

Archambeau, C. B., Flinn, E. A., and Lambert, D. G., 1969, Fine structure of the upper mantle, J. Geophys. Res., v. 74, p. 5825-5865.

Archambeau, C. B., Flinn, E. A., and Lambert, D. G., 1966, Detection, analysis and interpretation of teleseismic signals, 1. Compressional waves from the SALMON event, J. Geophys. Res., v. 73, p. 3877-3883.

Barazangi, M., Pennington, W., and Isacks, 1975, Global study of seismic wave attenuation in the upper mantle behind island arcs using pP waves, J. Geophys. Res., v. 80, p. 1079-1092.

Berzon, I. S., Passechnik, I. P., and Polikarpov, A. M., 1974, The determination of P-wave attenuation values in the Earth's mantle, Geophys. J. R. A. S., v. 39, p. 603-611.

Booth, D. C., Marshall, P. D., and Young, J. B., 1975, Long and short-period amplitudes from earthquakes in the range 0°-114°, Geophys. J. R. A. S., v. 39, p. 523-538.

Der, Z. A., Massé, R. P., and Gurski, J. P., 1975, Regional attenuation of short-period P and S waves in the United States, Geophys. J. R. A. S., v. 40, p. 85-106.

Frazier, C. W. and Filson, J., 1972, A direct measurement of Earth's short-period attenuation along a teleseismic ray path, J. Geopys. Res.,v. 77, p. 3782-3787.

Fuchs, K. and Müller, G., 1971, Computation of synthetic seismograms with the reflectionty method and comparison with observation, Geophys. J. R. Astr. Soc., v. 23, p. 417-433.

Gilbert, F. and Helmberger, D. V., 1972, Generalized ray theory for a layered sphere, Geophys. J. R. A. S., v. 27, p. 57-80.

Green, R. W. E. and Hales, A. L., 1968, The travel times of P waves to 30° in the central United States and upper mantle structure, Bull. Seism. Soc. Am., v. 58, p. 267-290.

Haskell, N. A., 1967, Analytic approximation for the elastic radiation from a contained nuclear explosion, J. Geophys. Res., v. 72, p. 2583.

REFERENCES (Continued)

Helmberger, D. V. and Wiggins, R. A., 1971, Upper mantle structure in mid-western United States, J. Geophys. Res., v. 76, p. 3229-3245.

Jordan, J. N., Mickey, W. V., Helterbran, W. and Clark, D. M., 1966, Travel times and amplitudes from the SALMON explosion, J. Geophys. Res., v. 71, p. 3469-3482.

Julian, B. R. and Anderson, D. L., 1968, Travel times, apparent velocities and amplitudes of body waves, Bull. Seism. Soc. Am., v. 58, p. 339-366.

Kanamori, H., 1967a, Spectrum of P and PcP in relation to the mantle-core boundary and attenuation in the mantle, J. Geophys. Res., v. 72, p. 559-571.

Kanamori, H., 1967b, Spectrum of short-period core phases in relation to the attenuation in the mantle, J. Geophys. Res., v. 72, p. 2182-2186.

Massé, R. P., 1973, Compressional velocity distribution beneath central and eastern North America, Bull. Seism. Soc. Am., v. 63, p. 911-935.

Noponen, I., 1975, Compressional wave power spectrum from seismic sources, Institute of Seismology, University of Helsinki, ISBN 951-45-0538-7. Contract AFOSR-72-2377 Final Report.

Patterson, D. W., 1966, Nuclear decoupling, full and partial, J. Geophys. Res., v. 71, p. 3427-3436.

Savino, J. M. and Archambeau, C. B., 1974, Discrimination of earthquakes from single and multiple explosions using spectrally defined event magnitude (Abstract), Transactions of the American Geophysical Union (EOS), v. 56, p. 1148.

Shumway, R. and Blandford, R., 1974, An examination of some new and classical short-period discriminants, SDAC-TR-74-10, Teledyne Geotech, Alexandria, Virginia.

REFERENCES (Continued)

Solomon, S. C. and Toksöz, M. N., 1970, Lateral variaiton of P and S waves beneath the United States, Bull. Seism. Soc. Am., v. 60, p. 819-838.

Springer, D. L., 1966, Calculation of first zone P wave amplitudes for SALMON event and for decoupled sources, J. Geophys. Res., v. 71, p. 3459-3467.

Trembly, L. D. and Berg, J. W., 1968, Seismic source characteristics from explosion-generated P waves, Bull. Seism. Soc. Am., v. 58, p. 1833-1848,

Veith, K. F. and Clawson, G. E., Magnitude from short-period P wave data, Bull. Seism. Soc. Am., v. 62, p. 435-452.

von Seggern, D. and Blandford, 1972, Source time functions and spectra for underground nuclear explosions, Geophys. J. R. A. S., v. 31, p. 83-97.

Wiggins, R. A. and Helmberger, D. V., 1973, Upper mantle structure of western United States, J. Geopys. Res., v. 78, p. 1870-1880.

Wiggins, R. A. and Helmberger, D. V., 1974, Synthetic seismogram computation by expansion in generalized rays, Geophys. J. R. A. S., v. 37, p. 73-90.

Wiggins, R. A. and Madrid, J. A., 1974, P wave train synthetic seismograms calculated by quantized ray theory, Geophys. J. R. A. S., v. 37, p. 407-422.

Yasar, T. and Nuttli, O. W., 1974, Structure of the shear-wave low-velocity channel in the western United States, Geophys. J. R. A. S., v. 37, p. 353-364.